Published in final edited form as:
*Nat Med*. 2017 May ; 23(5): 590–600. doi:10.1038/nm.4305.

# Thymosin α1 represents a potential potent single molecule-based therapy for cystic fibrosis

**Luigina Romani**[1,*], **Vasilis Oikonomou**[1], **Silvia Moretti**[1], **Rossana G. Iannitti**[1], **Maria Cristina D'Adamo**[2], **Valeria R. Villella**[3], **Marilena Pariano**[1], **Luigi Sforna**[1], **Monica Borghi**[1], **Marina M. Bellet**[1], **Francesca Fallarino**[1], **Maria Teresa Pallotta**[1], **Giuseppe Servillo**[1], **Eleonora Ferrari**[3], **Paolo Puccetti**[1], **Guido Kroemer**[4,5,6,7], **Mauro Pessia**[1,2], **Luigi Maiuri**[3,8], **Allan L. Goldstein**[9], and **Enrico Garaci**[10]

[1]Department of Experimental Medicine, University of Perugia, 06132 Perugia

[2]Department of Physiology and Biochemistry, Faculty of Medicine and Surgery, University of Malta, MSD 2080, Malta

[3]European Institute for Research in Cystic Fibrosis, Division of Genetics and Cell Biology, San Raffaele Scientific Institute, 20132 Milan, Italy

[4]INSERM U1138, Centre de Recherche des Cordeliers, INSERM U1138, Université Paris Descartes, Paris, France

[5]Metabolomics and Cell Biology Platforms, Institut Gustave Roussy, Villejuif, France

[6]Pôle de Biologie, Hôpital Européen Georges Pompidou, AP-HP; Paris, France

[7]Karolinska Institute, Department of Women's and Children's Health, Karolinska University Hospital, Stockholm, Sweden

[8]Department of Health Sciences, University of Piemonte Orientale, Novara, Italy

[9]Department of Biochemistry and Molecular Medicine, The George Washington University, School of Medicine and Health Sciences, Washington, DC

[10]University San Raffaele and IRCCS San Raffaele, 00166 Rome, Italy

## Abstract

Cystic fibrosis (CF) is caused by mutations in the gene encoding the cystic fibrosis transmembrane conductance regulator (CFTR) that compromise its chloride-channel activity. The most common



[*]**Corresponding Author:** Luigina Romani, M.D. (ORCID ID 0000-0002-1356-525X), Department of Experimental Medicine, University of Perugia, Piazz.le Gambuli, 06132 Perugia, Italy, Telephone and Fax: +39 075 585 8234, luigina.romani@unipg.it.

**Author Contribution**

V.O., R.G.I and M.P. performed most immunoblotting and immunofluorescence experiments; R.G.I., M.B., S.M. and E.F. performed murine in vivo experiments; M.C.D'A., L.S. and M.P. (Pessia) performed electrophysiology experiments; F.F. and M.T.P. performed TLR9 co-localization experiments; M.M.B. and G.S. performed transfection experiments; V.R.V. performed Ussing chamber experiments, A.L.G., L.M., G.K., M.P. (Pessia), P.P., E.G. and L.R. designed the experiments, analysed the data and wrote the paper.

**Competing Financial Interests**

A patent application by Luigina Romani and Enrico Garaci is pending (filing date, February 9, 2016, RM2015A000056 and 102015000053089).


Europe PMC Funders Author Manuscripts

mutation, p.Phe508del, results in the production of a misfolded CFTR protein, which has residual channel activity but is prematurely degraded. Because of the inherent complexity of the pathogenetic mechanisms involved in CF —which include impaired chloride permeability and persistent lung inflammation—a multidrug approach is required for efficacious CF therapy. To date, no individual, drug with pleiotropic beneficial effects for CF is available. Here we report on the ability of thymosin alpha 1 (Tα1)—a naturally occurring polypeptide with an excellent safety profile in the clinic when used as an adjuvant or an immunotherapeutic agent—to rectify the multiple tissue defects in CF mice as well as in cells from subjects with the p.Phe508del mutation. Tα1 displayed two combined properties that favorably opposed CF symptomatology; namely, it reduced inflammation and increased CFTR maturation, stability and activity. By virtue of this two-pronged action, Tα1 offers a strong potential to be an efficacious single molecule-based therapeutic agent in CF.

**Keywords**

Thymosin α1; inflammation; CFTR function

Cystic fibrosis (CF) is an autosomal recessive disorder caused by different mutations (see http://www.genet.sickkids.on.ca/cftr/StatisticsPage.html for a list) in the CF gene, encoding the cystic fibrosis transmembrane conductance regulator (CFTR) protein1. Presently, various pharmacological agents that target specific classes of CFTR mutation to address the basic defects, improve CFTR function and alter the disease process are available2. The p.Phe508del mutation in the first nucleotide-binding domain, which is the most common mutation among individuals with CF, results in the production of a misfolded protein with residual activity that is degraded by the ubiquitin-proteasome system during biogenesis2,3. Corrector drugs rescue trafficking of p.Phe508del-CFTR to the plasma-membrane (PM) by directly targeting the mutant protein2–4. However, in spite of their high efficacy in vitro, CFTR correctors show modest clinical benefits in individuals with CF harboring the p.Phe508del mutation, even when combined with the CFTR potentiator ivacaftor5,6. Given the complex molecular and cellular defects that occur in CF, a multidrug approach is desirable to both rescue and stabilize p.Phe508del-CFTR *in vivo*, and hence prevent the progressive decline of lung function in subjects with CF7. Recently, general strategies aimed at improving the proteostasis network by means of proteostasis regulators have emerged as an alternative approach to promoting the p.Phe508del-CFTR plasma-membrane (PM) targeting and stability8,9. Instead of directly targeting the mutant protein, proteostasis regulators favor p.Phe508del-CFTR rescue and stability by altering signaling pathways and checkpoints in cellular proteostasis8–10.

Optimal CF treatments should not only rescue CFTR localization and functionality, but also alleviate the associated hyperinflammatory pathology2,8. Rescuing chloride channel activity might be sufficient, *per se*, to reverse the inflammatory pathology in chronic CF lung disease11,12. However, the complexity of the p.Phe508del-CFTR molecular defect makes this task challenging. Irrespective of whether the inflammatory response is due to multiple, additive effects—including chronic infection—or is a primary outcome of CFTR dysfunction, a hyperinflammatory state in subjects with CF is associated, as a rule, with

early and nonresolving activation of innate immunity, which impairs microbial clearance and promotes a self-sustaining condition of progressive lung damage13. The remarkable persistence of chronic lung infections in the face of intensive antibiotic therapy14—and likewise, the major side effects of both corticosteroids15 and NSAIDs, including inhibition of the CFTR chloride-channel16—have revealed the need for approaches aimed at activating early anti-inflammatory pathways, to prevent, rather than correct, organ damage before patients become symptomatic. Moreover, hyperinflammatory mucosal responses to either cell-autonomous or environmental (e.g., bacterial) stresses can further compromise cellular proteostasis, thus affecting CFTR trafficking and function in a feed-forward loop10. Therefore, the ideal anti-inflammatory drug in CF should be one that interrupts the vicious CF cycle that sustains inflammation but also generates favorable conditions for CFTR trafficking. To date, no single drug is available with such positive pleiotropic effects in subjects with CF.

Thymosin alpha 1 (Tα1) is a naturally occurring polypeptide of 28 amino acids17, whose mechanism of action as an immune modulator presumably involves an ability to signal through innate immune receptors18, activated by dynamic association with membrane phosphatidylserine19. Tα1 (ZADAXIN®) is used worldwide as an immunomodulator in viral infections, immunodeficiencies, malignancies, and HIV/AIDS20. Owing to its ability to activate the tolerogenic pathway of tryptophan catabolism—via the immunoregulatory enzyme indoleamine 2,3-dioxygenase (IDO)121—Tα1 specifically potentiates immune tolerance in the lung, often breaking the vicious circle that perpetuates chronic lung inflammation in response to a variety of infectious *noxae*18. This led us to hypothesize that Tα1 could be beneficial in CF to alleviate early inflammation. Here we report that Tα1 is endowed with a unique property; namely, a dual ability to control inflammation and rectify functional defects of p.Phe508del-CFTR.

## Results

### Tα1 improves inflammation and immune tolerance in CF

Inflammation plays a critical role in lung disease development and progression in CF. IDO1, known to inhibit pathogenic Th17-cell activation and to initiate immune-tolerance mechanisms in the lungs21, is defective in subjects with the p.Phe508del-CFTR mutation22. Consistent with an ability to induce IDO1 via TLR9 signaling18, Tα1 promoted TLR9 co-localization in lysosomes (Fig. 1a), where maturation and signalling of TLR9 occur in response to stimulatory CpG oligodeoxynucleotides23. Concomitantly, Tα1 rescued defective IDO1 expression in an airway epithelial cell line (CFBE41o-) stably expressing p.Phe508del-CFTR24 (Fig. 1b). In doing so, Tα1 reduced pro-inflammatory NF-κB activity in response to the TLR-2 ligand MALP-2 (Fig. 1c,d) and promoted IRF3 phosphorylation and expression of the anti-inflammatory cytokine IL-10, (Fig. 1e), which are both known to contribute to immune tolerance in the lung18. Tα1 also rescued defective IDO1 expression, when administered in vivo to homozygous *F508del-Cftr* C57BL/6 mice ($Cftr^{F508del/F508del}$, hereafter referred to as $Cftr^{F508del}$ mice) infected with *Aspergillus fumigatus*, which colonizes CF airways and contributes to chronic lung disease25. Mice received Tα1 either intraperitoneally or intranasally (Supplementary Fig. 1a,b), soon after the infection or in an

established infection model (Supplementary Fig. 1c-e), daily for 6 days at 200 μg/kg, a dose previously shown to exert therapeutic activity in preclinical settings26 and to approximate, on a weight-per-weight basis, Tα1 doses that can be safely administered to humans27. Tα1 restored IDO1 expression both basally and after infection (Fig. 1f and Supplementary Fig. 1a) and concomitantly reduced caspase-1 cleavage (Fig. 1g) and NLRP3 expression (insets of Fig. 1h), thus reducing inflammasome activity. At the same time, it reduced lung pathology in naïve and infected mice (Fig. 1h and Supplementary Fig. 1d), fungal colonization (Fig. 1i and Supplementary Fig. 1c), and neutrophil infiltration (Fig. 1j and Supplementary Fig. 1b,e). The inflammatory cytokines TNF-α, IL-1β, and IL-17A were all reduced, and IL-10 as well as IL-1Ra increased by Tα1 (Fig. 1k and Supplementary Fig. 1b,e), which suggests that Tα1— via IDO1 induction—may also restrain pathogenic inflammasome activity in CF28. Similar results were obtained in *Cftr*$^{+/-}$ and *Cftr*$^{-/-}$ mice (Supplementary Fig. 2a-d), indicating that the anti-inflammatory activity of Tα1 occurs independently from CFTR expression and function. Tα1 also restrained inflammation and lung colonization in *Pseudomonas aeruginosa* infection (Supplementary Fig. 2e-g), indicating that it might favorably affect CF lung microbiology.

A limited but significant increase in body weight was afforded by Tα1 treatment (Supplementary Fig. 3a), and this prompted us to examine the effects of Tα1 on gut morphology in the mutant mice, also considering that loss-of-function mutations of *Cftr* cause a predominantly intestinal phenotype29. Similar to what was observed in the lung, Tα1 rescued IDO1 expression, tissue architecture, barrier function and cytokine balance in the small intestine of *Cftr*$^{F508del}$ mice (Supplementary Fig. 3b-e). This further suggested that Tα1, by impacting on CF inflammation and microbiology, favorably alters the natural history of the disease.

## Tα1 improves the localization and stability of mutant CFTR

Infection and inflammation may produce secondary alterations in CFTR expression and function30. This might predict that an efficient control of inflammation improves CFTR functioning. Considering that IDO1 is a potent driver of autophagy31, and that restoring disabled autophagy in CF will rescue CFTR function9,32, we interrogated whether Tα1 treatment would also affect CFTR functioning. We found that Tα1 favored trafficking of mature CFTR in CFBE41o- cells stably expressing p.Phe508del-CFTR. CFTR exit from the endoplasmic reticulum, passage through the Golgi, and delivery of the mature form (band C) to the cell surface are accompanied by an increase in molecular weight (from 135–140 to 170–180 kDa), as a result of glycosylation. At a clinically attainable dose33 , Tα1 increased cellular expression of mature p.Phe508del-CFTR (Fig. 2a; band C) by 10 ± 0.5 fold relative to vehicle-treated cells (Fig. 2b), reaching levels as high as 52 ± 7% of control values. The effect was observed at 30 min and up to 24 h (Fig. 2a), was dose-dependent (Fig. 2c), and still somewhat detectable at 24 h after Tα1 removal (Fig. 2d).

Low-temperature treatment of p.Phe508del airway cells alleviates the processing defect of the mutant protein, enhancing its PM localization34. Tα1 increased PM localization of p.Phe508del-CFTR to the half-maximal value afforded by low-temperature incubation (Fig. 2e,f), as revealed by immunoblotting of purified PM fractions (FLOT-1$^{+}$) with anti-CFTR

antibody (Fig. 2g,h) and immunofluorescence staining (Fig. 2i). We found clear restriction of p.Phe508del proteins around the nucleus in untreated CFBE41o- cells, as opposed to the mutated protein's migration to the PM after Tα1 treatment. This suggested that Tα1 increases the conformational stability of p.Phe508del-CFTR in the endoplasmic reticulum (ER), thus allowing its exit from ER and trafficking to the cell surface. This was confirmed by the limited proteolysis assay, which measures resistance to proteolytic digestion of folded *vs.* unfolded proteins35. Tα1 reduced the proteolytic digestion of p.Phe508del-CFTR (Fig. 2j).

As Rab GTPases modulate the intracellular trafficking of CFTR through the endosomal and recycling compartments36, we performed immunostaining of p.Phe508del-CFTR with markers of early (Rab5), late (Rab7), and recycling (Rab9) endosomes after Tα1 exposure. Tα1 reduced co-localization of mutant CFTR with Rab5 and Rab7, and it instead promoted co-localization with Rab9 (Fig. 2k), indicating that Tα1 reduces endocytic recycling through the early endosomes, prevents movement to the late endosomes and/or lysosomes, and favors recycling from endosomes to the PM. Thus Tα1 facilitates proper folding and trafficking of p.Phe508del-CFTR and also stabilizes the rescued CFTR mutant protein at the PM.

### Tα1 rescues CFTR protein through USP36-deubiquitination and autophagy

Next we measured the half-life of p.Phe508del-CFTR in CFBE41o- cells treated with Tα1 for 24 h at 37 °C. Tα1 did not increase steady-state CFTR mRNA expression (data not shown) and marginally affected the half-life of WT-CFTR, but it significantly increased the half-life of p.Phe508del-CFTR, which was shorter (1 h) than that of WT-CFTR (4 h) (Fig. 3 a,b). The effect of Tα1 could not be traced to inhibition of the proteasomal and lysosomal degradation pathways, as Tα1 did not inhibit degradation of reporter substrates (Supplementary Fig. 4a,b). However, Tα1 was detected in immunoprecipitated p.Phe508del-CFTR from CFBE41o- cells overexpressing Tα1 or treated with Tα1 for 2 h at 37 °C. While present in bronchial epithelial cells expressing WT-CFTR, Tα1 was not detected in immunoprecipitated WT-CFTR (Supplementary Fig. 5a,b). Overexpression of Tα1 increased CFTR maturation (Supplementary Fig. 5c), *IL10* expression and decreased *IL6* expression (Supplementary Fig. 5d), suggesting functional Tα1 activity. Consistent with the ER localization of Tα1 that is different from that of its precursor prothymosin37, these results indicated that Tα1 associates with p.Phe508del-CFTR, suggesting a chaperone activity of Tα1 that may affect the protein's ER quality control and degradation. Indeed, Tα1 perturbed the physical interaction of p.Phe508del-CFTR with the ER chaperon Hsp70, but not Hsp90 or calnexin, which are known to assist protein folding or degradation38 (Supplementary Fig. 5e,f).

Poorly-folded PM-bound CFTR is subjected to proteolysis by the ER-associated degradation mechanism via the cytosolic ubiquitin (Ub)-26S proteasome system. Ubiquitination was reduced in immunoprecipitated p.Phe508del-CFTR from CFBE41o- cells treated with Tα1 (Fig. 3c). Most of the ubiquitinated p.Phe508del-CFTR was ~200 kDa in molecular weight. Because CFTR detected by western blot was an ~180 kDa complex and a single ubiquitin

has a molecular mass of 8 kDa, it appears that Tα1 reduced multi-ubiquitination, a signal that targets proteins in early endosomes for lysosomal degradation.

The removal of ubiquitin by deubiquitinating enzymes (DUBs) regulates sorting of ubiquitinated PM-associated proteins39. Using a hemagglutinin-tagged ubiquitin probe engineered to form an irreversible, covalent bond with active DUBs35, we identified the ubiquitin-specific protease 36 (USP36)—which inhibits autophagy of protein aggregates by deubiquitination40—as a regulator of deubiquitination events triggered by Tα1. USP36—and neither of the two major p.Phe508del-CFTR DUBs, USP1035 and USP1941—could be detected in Tα1-treated cells (Fig. 3d). Paralleling the promotion of mature CFTR (Fig. 2), the induction of USP36 occurred at 30 min and was still present at 24 h of exposure (Fig. 3e). USP36 associated with immunoprecipitated p.Phe508del-CFTR (Fig. 3f) and deubiquitinated CFTR in $Rab5^+$ and more so $Rab9^+$ endosomes in Tα1-treated cells (Fig. 3g). This is in line with the finding that Rab9 enters the endosomal pathway at the transition stage between early $Rab5^+$ and late $Rab7^+$ endosomes and co-localizes to the trans-Golgi network42. The depletion of USP36 by RNA interference abrogated the rescuing effect of Tα1 on mature p.Phe508del-CFTR, while its over-expression further increased the capacity of Tα1 to rescue mutated CFTR (Fig. 3h). Thus the corrector activity of Tα1 correlated with USP36-mediated deubiquitination of CFTR in endosomes, thereby promoting its trafficking to the post-endocytic compartment and a more efficient ER export to the cell surface. USP36 was not involved in the promotion of IDO1 activity by Tα1 (Fig. 3i), a finding consistent with the importance of the proteasomal degradation pathway for IDO1 activity21, and likewise arguing for USP36 selectivity in CFTR correction.

The ubiquitin system is deeply influenced by autophagy43. Defective autophagy in CF leads to an increased pool of ubiquitinated proteins, including the ubiquitin-binding protein SQSTM1/p62, which is pivotal in the aggresome sequestration of ubiquitinated p.Phe508del-CFTR as well as in the p.Phe508del-CFTR disposal from PM after rescue32. Indeed, the enforced expression of SQSTM1/p62 lacking the UBA domain stabilizes p.Phe508del-CFTR at the PM and promotes its recycling10. Consistent with the ability of autophagy to rescue CFTR function9, Tα1 was able to promote IDO1-dependent autophagy (Supplementary Fig. 6a-d), to reduce SQSTM1/p62 levels (Supplementary Fig. 6e) and, importantly, to correct CFTR in an autophagy-dependent manner, as indicated by the decreased rescuing activity in mice bearing $Cftr^{F508del}$ in a $Becn1^{+/-}$ haploinsufficient background, which confers a major autophagy defect9 (Supplementary Fig. 6f).

## Tα1 increases p.Phe508del-CFTR and CLCA1 function

The corrector and stabilizing capacity of Tα1 would anticipate an increased chloride-ion channel function of the rescued p.Phe508del-CFTR. We treated p.Phe508del-CFTR-transfected CFBE41o- cells with Tα1 for 2 or 24 h at 37 °C before determining the channel open probability ($P_o$) of p.Phe508del-CFTR. Studies have estimated that the extent of correction in p.Phe508del airway epithelial cells must approximate 20–30% of WT CFTR function to provide therapeutic benefit44. Treatment with Tα1 for 2 h restored channel gating of rescued p.Phe508del-CFTR (Fig. 4a), with a 4-fold increase in $P_o$, namely, from 0.08 ± 0.02 of untreated CFTR to 0.35 ± 0.07 after treatment (Fig. 4b), with the latter $P_o$

values being similar to those in WT-CFTR45. A 2-fold increase in chloride-current density was still observed at 24 h, as assessed by whole-cell patch-clamp recordings of p.Phe508del-CFTR cells (Fig. 4c,d), and the rate of iodide efflux would then approximate 70% of the control value in WT cells, as assessed by the halide-sensitive fluorescent probe 6-methoxy-*N*-(sulphopropyl)quinolinium after stimulation with forskolin (Fig. 4e). This was confirmed by the results obtained in human bronchial epithelial (HBE) cells from a subject with two distinct—G1244E and p.Phe508del —mutations, whereby a gating defect46 occurred in association with the p.Phe508del defect. The effect of Tα1 was qualitatively similar, although of lesser extent, to that obtained with the potentiator ivacaftor (Fig. 4f), known to restore channel activity in CFTR gating (class III) mutations, including the G1244E mutation47. This in agreement with recent evidence indicating that proteostasis regulators rescue functional CFTR expression in human and mouse cells bearing only one copy of p.Phe508del9.

Bypassing CFTR by targeting additional ion channels is an alternative strategy to circumvent the CFTR defect48. Based on data gathered from DNA microarray analysis in vivo of Tα1-treated mice (Supplementary Fig. 7a,b), we assessed whether Tα1 would increase mRNA expression of the calcium-activated chloride channel regulator (CLCA)1, a member of the CLCA protein family capable of paracrine modulation of the activity of TMEM16A49, an alternative chloride channel that could obviate the primary defect in CF48. Tα1 potentiated calcium-activated chloride currents (Fig. 4g,h) and persistently increased the expression of *CLCA1* (Fig. 4i) in CFBE41o- cells. Depleting CLCA1 with specific siRNAs (Supplementary Fig. 7) greatly reduced the ion-channel activity promoted by Tα1 (Fig. 4e). These findings suggested that Tα1 is endowed with effects that can further ameliorate chloride-channel activity in CF.

## Tα1 rescues p.Phe508del-CFTR in mice and HBE cells

To determine whether Tα1 corrects CFTR *in vivo*, we assessed CFTR expression and activity in 4-wk-old $Cftr^{F508del}$ C57BL/6 mice treated daily for 6 days with 200 μg/kg Tα1. Tα1 restored CFTR expression in the lung (Fig. 5a,b) and small intestine (Fig. 5c,d), as assessed by immunoblotting of cell lysates (Fig. 5a,c), and it promoted localization of mature CFTR at the PM (Fig. 5b,d), as revealed by immunohistochemistry. Functionally, Tα1 treatment restored channel gating in lung epithelial cells with a 2-fold increase in $P_o$ from 0.23 ± 0.02 to 0.45 ± 0.04, before and after forskolin and genistein stimulation (Fig. 5e,f). In intestines from $Cftr^{F508del}$ mice mounted in Ussing chambers—much like the proteostasis regulator cysteamine9—Tα1 significantly increased CFTR-dependent $Cl^-$ conductance in response to forskolin (Fig. 5g). Rescuing of CFTR activity by Tα1 was also observed in $Cftr^{F508del}$ mice on an FVB/129 background (data not shown). Of interest, Tα1 also increased CLCA1 expression in both lung (Fig. 5h,i) and gut (Fig. 5j,k). Taken together, these data indicated that administration of Tα1 ameliorated $Cl^-$ fluxes in the intestinal and respiratory tracts of $Cftr^{F508del}$ mice.

To test the activity of Tα1 in a more relevant clinical setting, HBE cells from 5 subjects, homozygous for the p.Phe508del-CFTR mutation, were assessed for CFTR, USP36 protein levels and *CLCA1* gene expressions after exposure to Tα1 for 24 h at 37 °C. Tα1 increased

the expression of the mature p.Phe508del-CFTR (Fig. 6a), USP36 (Fig. 6b) and *CLCA1* (Fig. 6c) in 3 out of 5 subjects with CF and concomitantly increased ion-channel activity (Fig. 6d). To assess the clinical relevance of these findings, we measured the concentrations of Tα1 in sputa from subjects with the p.Phe508del-CFTR mutation and control subjects, considering that Tα1 is highly expressed not only in human thymic epithelium50 but also in peripheral tissues33. We found lower concentrations of Tα1 in subjects with CF than controls (Fig. 6e), which is consistent with the lower levels observed in supernatants and lysates from p.Phe508del-CFTR-transfected CFBE41o- cells relative to WT-CFTR–transfected cells (Fig. 6f). Because signaling via TLRs influences Tα1 production by lung epithelial cells (Supplementary Fig. 8), the deregulated TLR activity observed in subjects with CF13 may impact on local Tα1 production and, ultimately, CFTR activity. This likely occurs, as endogenous Tα1 affected CFTR functional expression. Indeed, we assessed mature CFTR expression in HBE cells from subjects with the p.Phe508del-CFTR mutation and controls after prothymosin depletion (by specific siRNA) or overexpression (via transfection), because Tα1 is produced by cleavage of prothymosin by the lysosomal asparaginyl endopeptidase legumain37. We found that mature p.Phe508del-CFTR expression was negated by prothymosin inhibition and increased by prothymosin overexpression (Fig. 6g). Of interest, prothymosin overexpression also increased mature CFTR expression in cells from controls (Fig. 6g), which points to a role for the endogenous prothymosin/Tα1 system in CFTR physiology.

We finally comparatively assessed the ion-channel activity of Tα1 with that of lumacaftor or ivacaftor, either alone or in combination, in primary HBE cells from controls or subjects homozygous for the p.Phe508del-CFTR mutation. Ussing chamber tracings revealed that Tα1 promoted the forskolin-induced increase in the chloride current (Isc) in HBE cells from subjects with CF (Fig. 6h) but not controls (Fig. 6i), an effect that was sensitive to CFTR inhibition and was similar to that observed with lumacaftor. With the only exception of subject #8 (Supplementary Fig. 9), the activity of Tα1 was not additive to ivacaftor, which is unable to rescue p.Phe508del-CFTR at the PM47. Similar results were obtained by means of a halide-sensitive fluorescent probe (Supplementary Fig. 9). In spite of the reported interindividual variability even in patients bearing the same genotype, these results suggest that Tα1 alone or in combination can be used for treating subjects with the p.Phe508del-CFTR mutation.

## Discussion

While regulation of lung homeostasis and inflammation by CFTR is an established notion51, whether regulation of inflammation will impact on CFTR functioning is less clear. Here we show that Tα1 is endowed with the unique activity to correct CFTR defects through regulation of inflammation. Although Tα1 appears to have a multitasking chaperon activity through which it may affect the balance of protein folding *vs.* degradation (e.g., by associating with p.Phe508del-CFTR, perturbing the interaction of mutated CFTR with the ER chaperons, and activating USP36-mediated deubiquitination of misfolded CFTR), the induction of IDO1 appears to be key to this mechanism. IDO1 is known to play a major role in preventing excessive pathology in immune-mediated tissue injury through multiple effector mechanisms, including the induction of autophagy31. Consistent with the ability of

autophagy to rescue CFTR function9, the promotion of autophagy appeared to contribute to the corrector activity of Tα1 and qualified Tα1 as a proteostasis regulator that rectifies an unbalanced degradasome activity in CF cells. Proteostasis regulators, such as cysteamine, have emerged as a new option for CFTR repair by avoiding unwanted protein-protein interactions, favoring trafficking and stability of mutant CFTR, and hence controlling inflammation9,10,32. Unlike cysteamine, the anti-inflammatory effects of Tα1 are not dependent on an ability to rescue a functional p.Phe508del-CFTR, as they also occur in CFTR knockout mice. Therefore, Tα1 is an excellent example of a drug with primary anti-inflammatory effects that can also favor rescuing of p.Phe508del-CFTR.

The cross-regulation between autophagy and inflammasomes52 may also explain the ability of Tα1 to inhibit NLRP3-based inflammasome activity, known to contribute to respiratory infections and pathologic airway inflammation in CF28. Moreover, as immune tolerance induced by IDO1 encompasses an activity on tissue repair and remodeling53, this may explain the remarkable effect of Tα1 in restoring host-tissue architecture in the lung and the GI tract of *Cftr*$^{F508del}$ mice. Similar to subjects with CF30, an altered pulmonary histopathophysiology is present in those mice in the absence of infection54. All together, these findings may point to Tα1 as a drug candidate capable of preventing disease progression at very early stages.

Through its multitasking activity, Tα1 may represent a proper means of rectifying the multifunctional defect in individuals with CF, including the increase in CLCA1 activity. Both clinical and animal-model studies have suggested a compensatory role for CLCA1 in CF55,56. Even though calcium-activated chloride channels are abundant in mouse but not in human airways48,57, mutations in CLCA1 are found in a subset of individuals with CF marked by aggravated intestinal disease55, a finding consistent with the observation that calcium-activated chloride channels are defective in the intestine of individuals with CF57. This may explain the remarkable activity of Tα1 in the GI tract of *Cftr*$^{F508del}$ mice, in which chloride-channel activity was rectified. This indicates that Tα1 could be clinically exploited for pharmacologic correction of defective CFTR not only in the lung but also in the gut, implicating that gastrointestinal outcome measures could be promising clinical endpoints of Tα1 therapeutics.

Only a combination of molecules with different mechanisms of action is expected to induce a significant degree of p.Phe508del-CFTR correction, as shown by the combination of ivacaftor with lumacaftor6,58 or VX-66159,60. Although the corrector activity of Tα1 has yet to be verified relative to the agents moving into development in the clinic, the excellent safety profile and cost effectiveness of ZADAXIN® in adults and children20 suggest that Tα1 could be tested in clinical trials for possible pulmonary and extra-pulmonary benefits in individuals with CF.

## Online Methods

### General experimental approaches

Sample size was chosen empirically based on our previous experiences in the calculation of experimental variability; no statistical method was used to predetermine sample size and no

samples, mice or data points were excluded from the reported analyses. Experimental groups were balanced in terms of animal age, sex and weight. No blinding was applied upon harvesting samples after the treatments.

## Mice

Murine experiments were performed according to the Italian Approved Animal Welfare Authorization 360/2015-PR and Legislative decree 26/2014 regarding the animal license obtained by the Italian Ministry of Health lasting for five years (2015-2020). Infections were performed under isoflurane anesthesia, and all efforts were made to minimize suffering. CF mice homozygous for the F508del-CFTR which had been backcrossed for 12 generations to the C57BL/6 strain, or in the FVB/129 outbred background (*Cftr* $^{tm1EUR}$, F508del, abbreviated *Cftr* $^{F508del/F508del}$) were obtained from Bob Scholte, Erasmus Medical Center Rotterdam, The Netherlands61. *Cftr*$^{F508del/+}$ female mice were backcrossed to the C57BL/6 background *Becn1*$^{+/-}$ male mice to obtain *Becn1* haploinsufficient *F508del* homozygous mice (abbreviated *Cftr*$^{F508del/F508del}$/*Becn1*$^{+/-}$), as described62. These mice were provided with a special food, consisting of an equal mixture of SRM-A (Arie Blok, Woerden, The Netherlands) and Teklad 2019 (Harlan Laboratories, San Pietro al Natisone, Udine, Italy) and water acidified to pH 2.0 with HCl and containing 60 g/l PEG 3350, 1.46 g/l NaCl, 0.745 g/l KCl, 1.68 g/l $NaHCO_3$ and 5.68 g/l $Na_2SO_4$. Newborn mice were genotyped by cutting a small piece of tail 12 days after birth. Four to six-week C57BL/6 mice purchased from Charles River (Calco, Italy) and genetically engineered homozygote KO *Cftr* mice (B6.129P2-KO *Cftr*$^{tm1UNC}$, abbreviated *Cftr*$^{-/-}$ and *Cftr*$^{+/-}$ mice, gut-corrected, on C57BL/6 background were bred under specific pathogen-free conditions at the Animal Facility of San Raffaele Hospital, Milan Italy. Male and female mice were used in all studies.

## Infections and treatments

Mice were anesthetized in a plastic cage by inhalation of 3% isoflurane (Forane Abbot) in oxygen before intranasal instillation of 2 x $10^7$ *A. fumigatus* (Af293) resting conidia/20 μl saline. For *Pseudomonas aeruginosa* infection, appropriate dilutions with sterile PBS were made to prepare the inoculum before intranasal instillation of 3 x $10^7$ CFU/mice63. Quantification of microbial growth was done as described63. For histology, paraffin-embedded sections were stained with Periodic acid-Schiff (PAS) and hematoxylin and eosin (H&E). Mice were treated either intraperitoneally (i.p.) or intranasally (i.n.) with Tα1 or the scrambled polypeptide reconstituted in sterile water (200 μg/kg in 20 μl saline (i.n.), or 100 μl saline (i.p.) given daily for 6 consecutive days in uninfected mice and either beginning the day of the infection or starting 7 days after the infection. Mice were weighed on the first and last day of the treatment. Mice were gavaged with cysteamine (60 μg/kg in 100 μl saline/day) for 6 days as reported64. For BAL fluid collection, lungs were filled thoroughly with 1-ml aliquots of pyrogen-free saline through a 22-gauge bead-tipped feeding needle introduced into the trachea. Bronchoalveolar lavage (BAL) fluid was collected in a plastic tube on ice and centrifuged at 400 × *g* at 4°C for 5 min. For differential BAL fluid cell counts, cytospin preparations were made and stained with May-Grünwald Giemsa reagents (Sigma-Aldrich). At least 200 cells/field/10 fields were counted, and the absolute number of neutrophils was calculated. For epithelial cells purification, lung epithelial cells, at 99% expressing cytokeratin, on pan–cytokeratin antibody staining of cytocentrifuge preparations, and >90%

viable on trypan blue exclusion assay, were isolated as described65. Cells were stimulated with MALP-2, Poly (I:C), ultrapure lipopolysaccharide from *Salmonella minnesota* Re 595 (all from Sigma-Aldrich), and CpG oligodeoxynucleotides **(**ODN) (all at 10 μg/ml) for 1 h (NF-κB and IRF3, protein expression) or 4 h (*IL10* gene expression). Uncropped immunoblots are shown in Supplementary Information.

## Cells

Human Bronchial Epithelial (HBE) cells, homozygous for the p.Phe508del mutation and its isogenic wild-type were obtained from lung transplants (individuals with CF) or lung resections (Controls) (kindly provided by LJ Galietta within the Italian Cystic Fibrosis Foundation). Cells were maintained at 37°C in a humidified incubator in an atmosphere containing 5% $CO_2$, and the experiments were done 5 days after plating66. Stable lentiviral-based transduction of the parental CFBE41o- cells, homozygous for the p.Phe508del-CFTR mutation67, with either WT-CFTR or p.Phe508del-CFTR were provided by LJ Galietta. The transduced CFBE41o-cells were maintained in minimum Eagle's medium supplemented with 50 units/ml penicillin, 50 μg/ml streptomycin, 2 mM L-glutamine, 10% fetal bovine serum, and 1 μg/ml blasticidine (WT-CFTR) or 2 μg/ml puromycin (p.Phe508del-CFTR) in a 5% $CO_2$, 95% air incubator at 37 °C. To establish polarized monolayers, CFBE41o- cells were seeded on 24-mm-diameter Transwell permeable supports (0.4 mm pore size; Corning Corp., Corning, NY) at $2 \times 10^6$ and grown in air-liquid interface culture at 37 °C for 6-9 days and then at 27°C for 36 h. Cells were incubated with different concentrations of Tα1 (CRIBI Biotechnology), 3 μM VX-809 (Lumacaftor, Aurogene), 1μM VX-770 (Ivacaftor, Aurogene) alone or in combination for up to 24 h before the assessment of CFTR protein expression and function at either 37 °C or 26 °C. For washout experiments, after treatment period the medium was replaced with complete medium for the indicated time. DMSO vehicle alone (0.1%, v/v) was used as a control. Tα1 and the scrambled polypeptide were supplied as purified (the endotoxin levels were <0.03 pg/ml, by a standard limulus lysate assay) sterile, lyophilized, acetylated polypeptide. The sequences were as follows: Ac-Ser-Asp-Ala-Ala-Val-Asp-Thr-Ser-Ser-Glu-Ile-Thr-Thr-Lys-Asp-Leu-Lys-Glu-Lys-Lys-Glu-Val-Val-Glu-Glu-Ala-Glu-Asn-O (Tα1) (SEQ ID NO:1) and Ac-Ala-Lys-Ser-Asp-Val-Lys-Ala-Glu-Thr-Ser-Ser-Glu-Ile-Asp-Thr-Thr-Glu-Leu-Asp-Glu-Lys-Val-Glu-Val-Lys-Ala-Asn-Glu-OH (scrambled peptide) (SEQ ID NO:2). For cell cultures, CFBE41o-cells were stimulated with CpG ODN (10 μg/ml) or MALP-2 (100 ng/ml) with/without 100 ng/ml of Tα1 for 2 h and then lysed for immunoblotting or assessed for cytokine analysis by RT-PCR. Recombinant IFN-γ, from Santa Cruz Biotechnology, was used at the concentration of 10 ng/ml. HEK-293 cells were maintained in DMEM supplemented with 50 units/ml penicillin, 50 μg/ml streptomycin, 2 mM L-glutamine and 10% fetal bovine serum in a 5% $CO_2$, 95% air incubator at 37°C. Regular testing for mycoplasma contamination was carried out by PCR. Human studies approval was obtained from institutional review boards at each site and written informed consent was obtained from the participants, or, in case of minors, from parents or guardian.

## Immunofluorescence and immunohistochemistry

CFBE41o-cells were treated with 100 ng/ml Tα1 at 37°C for 24 h, fixed in 2% formaldehyde for 15 min at room temperature and permeabilized in a blocking buffer

containing 5% FBS, 3% BSA, and 0.5% Triton X-100 in PBS. The cells were then incubated at 4°C with the primary antibody anti-CFTR (clone CF3, Abcam). After extensive washing with PBS, the slides were then incubated at room temperature for 60 min with goat anti-mouse antibody to CFTR followed by Alexa Fluor 555 (Clone Poly4053, Biolegend) and Alexa Fluor 488 anti-Phalloidin (A12379, Thermo Fisher) for F-actin labelin. For intracellular routing, cells were plated in complete medium into chambered coverglass (Lab-Tek/Nunc; Thermo Scientific) in a temperature-regulated environmental chamber and exposed to 100 ng/ml Tα1 at 37°C for 2 h, in serum free RPMI-1640 medium. After washout, cells were fixed, permeabilized and incubated at 4°C with primary antibodies anti-Rab5, anti-Rab7, anti-Rab9 (all from Sigma) and anti-USP36 (clone 7G3, Abcam). After extensive washing with PBS, the cells were incubated at room temperature for 60 min with 1:400 secondary anti-rabbit IgG–FITC antibody (Sigma-Aldrich). For TLR9 co-localization, HEK 293 cells transfected with the human TLR9 tagged at its C-terminus with enhanced green fluorescent protein (TLR9-GFP) was obtained from Prof. Giuseppe Teti, University of Messina, Italy. Cells were seeded onto sterilized coverslip placed in a 6-well plate and stimulated with 1 μg/ml CpG ODN in the presence of 100 ng/ml Tα1 for 30 min. Cells were then fixed with 4% paraformaldehyde, permeabilized by 0.1% Triton X-100 and stained with biotin anti-human CD107a antibody (Biolegend) for the Lysosomal-associated membrane protein 1 (LAMP-1) or with biotin anti-transferrin receptor antibody (DF1513, Abcam) and revealed by Streptavidin, Alexa Fluor® 568 conjugate (ThermoFisher). The tissues were removed and fixed in 10% phosphate-buffered formalin, embedded in paraffin and sectioned at 5 μm. Sections were then rehydrated and after antigen retrieval in citrate buffer (10 mM, pH 6.0), sections were fixed in 2% formaldehyde for 40 min at room temperature and permeabilized in a blocking buffer containing 5% FBS, 3% BSA, and 0.5% Triton X-100 in PBS. The sections were incubated at 4 °C with primary antibodies anti-NLRP3 (ab4207, Abcam) over night and then incubated at room temperature for 60 min with secondary antibodies, for NLRP3 goat anti-mouse Alexa Fluor 555 (Clone Poly4053 Biolegend). For immunohistochemistry, sections were incubated overnight with anti-CFTR (clone CF3, Novus) or anti-CLCA1 (Abcam) followed by biotinylated secondary antibodies. Cells were counterstained with hematoxylin or DAPI to detect nuclei. All images were acquired using a fluorescence microscope BX51 Olympus with a ×20, ×40 and ×100 objective with the analySIS image processing software (Olympus).

### Western blot analysis and immunoprecipitation

Blots of cell lysates were incubated with antibodies against the following proteins: CFTR (clone CF3 from Abcam, clone CF3 from Novus and clone 2269 from Cell signaling), anti-CLCA1 (Abcam), anti-USP36 (Proteintech), monoclonal anti-murine IDO1 antibody (cv152)68, anti-human IDO1 (clone 10.1, Millipore), anti-phospho-NF-κB/p65 and anti-NF-κB/p65 (Cell Signaling), anti-phospho-IRF3 (Cell Signaling) and anti-IRF3 (Santa Cruz). For immunoprecipitation, cells were lysed in immunoprecipitation buffer containing 150 mM Sodium Chloride (NaCl), 50 mM Tris (pH 8.0), 1% Triton-X100, 0.5% Sodium deoxycholate, 0.1% Sodium dodecylsulphate (SDS), Complete Protease Inhibitor Cocktail (Roche), and PMSF (Roche). CFTR and IDO1 were immunoprecipitated by incubation with 1 μg of the specific antibody. The reaction was performed overnight and either Protein A (for CFTR) or Protein G (IDO1) Sepharose 4 Fast Flow (GE Healthcare) were added and

incubated for additional 2 h. Beads were washed and resuspended in Laemmli buffer. Immunoprecipitated proteins were separated by SDS-PAGE and immunoblots were probed with anti-USP36, anti-Hsp70, anti-Hsp90, anti-Calnexin and anti-Ubiquitin antibody that recognizes mono, oligo or polyubiquitinated additions (all from Abcam). For physical association of Tα1 to CFTR, immunoprecipitated proteins were separated by Tricine-SDS-PAGE69 and immunoblots were probed with anti-Thymosin alpha 1 antibody (ab76557, Abcam). Normalization was performed probing the membrane with β-actin or β-tubulin antibody (clone AC-15 or clone TUB 2.1, Sigma). Alternatively, lysates from HEK-293 cells transfected with FLAG-Tα1 were immunoprecipitated using an affinity resin with anti-Flag M2 (clone M2, Sigma) and the resulting FLAG-Tα1-resin was then incubated in the presence of lysates from CFBE41o- cells transfected with WT-CFTR or p.Phe508del-CFTR. Samples were resolved by immunoblotting and probed with anti-CFTR antibody. Lysates from p.Phe508del-CFTR CFBE41o-cells were transfected with FLAG-Tα1 and immunoprecipitated using the affinity resin with anti-FLAG M2. In order to avoid non-specific binding, after elution with Flag peptide (Sigma), the remaining proteins bound to the resin were loaded as negative control. Samples were resolved by immunoblotting and probed with anti-CFTR antibody. Chemiluminescence detection was performed with LiteAblotPlus chemiluminescence substrate (Euroclone S.p.A), using the ChemiDocTM XRS+Imaging system (Bio-Rad), and quantification was obtained by densitometry image analysis using Image Lab 5.1 software (Bio-Rad). Uncropped immunoblots are shown in Supplementary Information.

## Luciferase assay

CFBE41o-cells were seeded in 24-well plates at a density of 7.5 x $10^4$ cells per well. Cells were transfected using Lipofectamine 2000 (Invitrogen) according to the manufacturer's protocol. Each transfection contained 100 ng of a luciferase reporter plasmid (pLV-5X-NF-κB-RE Luc) and 50 ng of a β-galactosidase internal control reporter plasmid (pGL3-lacZ), with or without MALP-2 (100 ng/ml). The total amount of DNA applied per well was adjusted to 600 ng by adding pCDNA3 empty vector (ev). Cells extracts were subjected to a luminometry-based luciferase assay and luciferase activity was normalized by β-galactosidase activity.

## Membrane fractionation

Cells were homogenized with a Potter-Elvehjem pestle and centrifuged at 2300 x g for 15 min at 4°C. Supernatant fractions that contain the cytoplasmic and plasma membrane fractions were centrifuged 1 h at 16,000 x g at 4°C; the pellet was the intact membrane and was solubilized in Buffer A (20 mM Tris-HCl, pH 7.4, 2 mM EDTA, 20 mM 2-mercaptoethanol, 1X PMSF, 1 mg/ml inhibitor protease cocktail (P8340, Sigma) 0,1% Triton X-100 (X-100-RS, Sigma) and centrifuged 1 h at 60,000 x g in the ultracentrifuge. The supernatant fractions were collected as plasma membrane fraction and proteins were separated by SDS-PAGE and immunoblots were probed with anti-CFTR (Cell Signaling) and anti-Flotillin 1 antibody (Sigma). Uncropped immunoblots are shown in Supplementary Information.

### CFTR half-life

Cycloheximide, (CHX, 40 μg/ml), was added on CFBE41o-cells treated with 100 ng/ml Tα1 for 24 h at 37°C, for up to 6 h. Cell lysates were assessed for CFTR protein expression by western blotting. Uncropped immunoblots are shown in Supplementary Information.

### Proteasome and lysosome assays

CFBE41o-cells were plated on a 12-well cell culture plate and stimulated with Tα1 (100 ng/ml) for 2 h at 37°C. For proteasome activity, cells were lysed with NP-40 lysis buffer and the amount of pmols of proteolytic activity was analysed with the proteasome activity assay kit (Abcam) that takes advantage of the chymotrypsin-like activity, utilizing an AMC-tagged peptide substrate (Succ-LLVY-AMC), which releases free, highly fluorescent AMC in the presence of proteolytic activity. For lysosomal activity the Lysosome/Cytotoxicity Dual Staining Kit (Abcam) was used as per manufacturer's instructions.

### Limited Proteolysis of CFTR

CFBE41o-cells were treated for 2 h at 37°C and lysed in PBS-Triton X-100 (0.1%) for 1 h at 4°C. Lysates were cleared by centrifugation at 20,000 rpm for 10 min in a Beckman Allegra 64R centrifuge. Supernatants were removed, and total proteins were determined by Quant-iT™ Protein Assay Kit (Thermo Scientifics) following manufacture's instructions. Cell lysates were then diluted to a concentration of 20 μg/ml, and trypsin was added at the indicated final concentrations. The cleavage reactions were incubated on ice for 15 min and were then quenched by addition of complete protease inhibitor (Roche) and trypsin inhibitor. Sample buffer was added to a final 1× concentration, and samples were run on 7% SDS–PAGE gels. Uncropped immunoblots are shown in Supplementary Information.

### Identification of active DUBs

CFBE41o- cells were lysed in the immunoprecipitation assay buffer (25 mM Tris-HCl, pH 7.6, 10 mM NaCl, 1% Triton X-100, 1% sodium deoxycholate, 0.1% SDS), and 0.1 μg of the HA-UbVME probe (Enzo) was added to 20 μg of protein extract. HA-UbVME probe forms an irreversible, covalent bond with active DUBs. Identification of DUBs covalently linked to the HA-UbVME probe was achieved by immunoprecipitation of the HA-UbVME DUB complex(s) using an anti-HA antibody (A190-108A, Bethyl Laboratories) followed by SDS-PAGE and Western blot analysis using specific anti-DUB antibodies USP19 (Bethyl Laboratories), USP10 (Bethyl Laboratories) and USP36 (Proteintech). The specificity of the HA-UbVME probe for active DUBs was confirmed with the addition of N-ethylmaleimide (10 μM) to inhibit cysteine protease DUBs, during the labeling reaction. Uncropped immunoblots are shown in Supplementary Information.

### Plasmids and transfection

The Flag-HA-USP36 plasmid a gift from Wade Harper (Addgene plasmid # 22579)70 was used for transfection experiments. For the generation of the plasmid incoding pcDNA™3.1/myc-His with the prothymosin α (*PTMA*) fragment, the CDS *PTMA* cDNA was amplified by PCR with its specific primers containing EcoRl and XhoI anchorettes. The fragment was then subcloned into the EcoRl and XhoI cloning site of the pcDNA™3.1/myc-His A

(Thermo Fisher Scientific, Waltham, MA) to construct the recombinant pcDNA™3.1/myc-His-PTMA expression vector. To isolate the sequence encoding the Tα1 active peptide, cDNA sequence corresponding to Tα1 was amplified by PCR with its specific primers containing EcoRI and XhoI anchorettes, using *PTMA* pCDNA3.1/myc-Hys A as template, and cloned into expression vector pCMV-Tag 2B (Agilent Technologies, Santa Clara, CA). Transient transfections were performed with a pCMV expressing FLAG-Tα1 using TransIT® Transfection Reagent (Mirus), according to manufacturer's instruction, in HEK-293 cells and HBE F508-del cells incubated for 24 h at 37°C in 5% $CO_2$. The empty vector was performed as a negative control.

### RNA interference

The Integrated DNA technologies-pool duplexes of predesigned siRNA (*USP36*, duplex name: MMC.RNAI.N007887.12.1, *CLCA1* duplex name: MMC.RNAI.N001285.12.1) were purchased from IDT (TEMA Ricerca). Specific SiRNA towards prothymosin α was purchased from Sigma. For SiRNA delivery, cells were incubated for 24 h (as indicated by preliminary experiments performed at 12, 24, or 48 h) at 37°C in 5% $CO_2$ with specific SiRNA using the TransIT-TKO® Transfection Reagent (Mirus) following the manufactures instructions. Effectiveness of silencing of specific targets was verified by evaluating target mRNA level using real-time quantitative PCR (Supplementary Fig. 8d) and protein expression by western blotting (Fig. 3g and Fig. 6g).

### Autophagy

RAW 264.7 cells (ATCC) were seeded in 100-mm petri dish ($3.5 \times 10^6$) and transfected with the EGFP-LC3 plasmid (Addgene) using ExGen 500 in vitro Transfection Reagent (Fermentas) for 48 hours, according to the manufacturer's instructions. Transiently transfected RAW 264.7 cells or HBE cells from CF patients with the p.Phe508del mutation were exposed to 1 or 100 ng/ml of Tα1 for 4 h at 37°C in 5% $CO_2$, as described71. Cultures growing on coverslips were observed at ×100 magnification with the Olympus BX51 fluorescence microscope using an FITC filter. Results are expressed as number of cells with EGFP-LC3 puncta. An equal amount of cell lysate in 2× Laemmli buffer (Sigma) was probed with rabbit anti-LC3B (Cell Signaling) and goat anti-rabbit IgG HRP-conjugated secondary antibody (Sigma) or anti-Beclin-1 (Cell Signaling) and anti-SQSTM1/p62 (Cell Signalling) antibody. Normalization was performed by probing the membrane with anti–β-tubulin antibody (Sigma). Alveolar macrophages from C57BL/6 and $Indo^{-/-}$ lung cells were isolated after 2-hour plastic adherence at 37°C and treated with Tα1 as described above before the assessment of LC3 expression by immunofluorescence. Chemiluminescence detection was performed with LiteAblot Plus chemiluminescence substrate (EuroClone), using the ChemiDoc XRS+ imaging system (Bio-Rad), and quantification was obtained by densitometry image analysis using Image Lab 5.1 software (Bio-Rad). Uncropped immunoblots are shown in Supplementary Information.

### Functional analysis of CFTR and calcium-activated chloride currents

Patch-clamp recordings were performed from p.Phe508del-CFTR-transfected CFBE41o- cells (treated with 100 ng/ml Tα1 for 2 or 24 h at 37 °C) and from bronchial epithelial cells derived from $Cftr^{F508del}$ C57BL/6 mice. CFTR single-channel activity was measured at

25°C by means of the on-cell configuration, using an Axopatch 200B amplifier (Axon Instruments). Both, the pipette and bath solutions contained (in mM): 140 N-Methyl-D-glucamine, 5 $CaCl_2$, 2 $MgSO_4$, and 10 TES (adjusted to pH 7.30 with HCl), total $[Cl^-]o$=140 mM. Seal resistances ranging from 5 to 20GΩ were obtained. The membrane potential was maintained at -40 mV and pulses from −100 to +100 mV, lasting 5s, were delivered. Pipettes with resistance of 5–10 MΩ were pulled from borosilicate glass capillary tubing (GC150-F10; Clark Electromedical Inc.), using a two-step horizontal puller from Sutter Instrument (U.S.A.). Cells were stimulated with forskolin (Fsk, 10 μM) and genisteine (Gen, 30 μM). Single-channel recordings were sampled at 5 kHz and filtered at 200 Hz with an eight-pole Bessel filter. Macroscopic CFTR and calcium-activated chloride currents were recorded by means of the whole-cell configuration, using an EPC-10 patch-clamp amplifier (HEKA Elektronik, Germany). I–V relationships were built by clamping the membrane potential of CFBE41o-cells at -40mV and by delivering ramps from -100mV to 50mV. The pipette solution contained (mM): 113 L-aspartic acid, 113 CsOH, 27 CsCl, 1 NaCl, 1 $MgCl_2$, 1 EGTA, 10 TES (pH 7.2). MgATP (3mM) was added just before patch-clamp experiments were started. The external solution contained (mM): 145 NaCl, 4 CsCl, 1 $CaCl_2$, 10 glucose, 10 TES (pH 7.4). Results were analyzed with PATCHMASTER software (HEKA Elektronik).

The colorimetric assay with the SPQ (6-methoxy-N-(3-sulfopropyl) quinolinium) fluorescent probe (Molecular Probes/Invitrogen)72 was also used to estimate CFTR channel activity. Briefly, the iodide-sensitive fluorescent indicator SPQ was introduced into the cells in a hypotonic solution of iodide buffer (in mM: 130 NaI, 4 $KNO_3$, 1 $Ca(NO_3)_2$, 1 $Mg(NO_3)_2$, all from Sigma Aldrich, 10 glucose and 20 HEPES, pH 7.4) diluted 1:1 with water and containing a final concentration of 10 mM SPQ. Cells were loaded for 20 min at 37°C in a humidified chamber with 5% $CO_2$. The SPQ-loaded cells were assessed with TECAN (Thermo Fisher Scientific) plate reader with a 37°C heated stage and perfused with iodide buffer for 5 to 8 min. Changes in CFTR-mediated SPQ fluorescence were monitored at the 445 nm wavelength in response to excitation at 340 nm during perfusion at 37°C in nitrate buffer replaced with 130 mM $NaNO_3$ with 20 μM forskolin plus 100 μM IBMX (all from Sigma Aldrich) and fluorescence intensity measured for a further 10 to 12 min. Signals were collected at 30-sec interval. For each minute, the average of the fluorescence intensity was measured from 50 cells for population per coverslip and the peak of iodide efflux rate (usually after Fsk plus IBMX adding) of cells was calculated in accordance with the Stern-Volmer relationship as follows: (Fo/F)-1= KCQ where F is the observed fluorescence, Fo is the fluorescence in the absence of a quenching anion, CQ is the concentration of the quenching anion, and K is the Stern-Volmer quench constant.

### Preparation of RNA and microarray hybridization

Total lung RNA was extracted using Trizol reagent (Life Technologies). Integrity of total RNA was evaluated using the Agilent Bioanalyzer 2100 system (Agilent Technologies) and was within RNA integrity number 7 to 9 and thus considered suitable for further processing. 100 ng of total RNA were processed to produce fragmented biotin-labeled cDNA using the GeneChip® WT PLUS Reagent Kit according to manufacturer's instructions. Samples were hybridized to Affymetrix GeneChip Mouse Gene 2.0 ST arrays and quantified. Images were

processed and cell intensity files (CEL files) were generated in the GeneChip Command Console Software (Affymetrix). CEL files were processed using Expression Console v. 1.4.1.46 to yield RMA summarized $Log_2$ transformed expression values for probe sets (CHP files). Normalized expression data (CHP files) were analyzed using Transcriptome Analysis Console Software (Affymetrix) and ANOVA in R using R package Bioconductor.

### Ussing chamber

Chambers for mounting tissue biopsy were obtained from Physiologic Instruments (model P2300, San Diego, CA, USA). Chamber solution was buffered by bubbling with a mixture of 95% $O_2$ and 5% $CO_2$. Tissues were short circuited using Ag/AgCl agar electrodes. Short-circuit current and resistance were acquired or calculated using the VCC-600 transepithelial clamp from Physiologic Instruments and the Acquire & Analyze 2.3 software for data acquisition (Physiologic Instruments), as previously described62. A basolateral-to-apical chloride gradient was established by replacing NaCl with Na-gluconate in the apical (luminal) compartment to create a driving force for CFTR-dependent $Cl^-$ secretion. CFTR channels present at the apical surface of the epithelium (lumen side of the tissue) were activated.Stimulations with forskolin, CFTR inhibitor 172 and amiloride were as described62.

### ELISA and real-time PCR

The levels of cytokines were determined by specific ELISAs (R&D Systems). For Tα1 production (ELISA kit from Immundiagnostik) either cell culture supernatants or cell lysates were used. Real-time RT-PCR was performed using the BioRad CFX96 System and SYBR Green chemistry (BioRad). The PCR primers were as follow: *IL10* Forward, 5′-GCCTAACATGCTTCGAGATC -3′ and Reverse, 5′- TGATGTCTGGGTCTTGGTTC -3′; *IL6* Forward, 5′- CCACTCACCTCTTCAGAACGAATT -3′ and Reverse, 5′-AGTGCCTCTTTGCTGCTTTCA -3′; *CLCA1* Forward, 5′-GCTGATGTTCTGGTTGCTGA -3′ and Reverse, 5′- CGTCAAATACTCCCCATCGT -3′; *Cldn1* Forward, 5′-AGCCAGGAGCCTCGCCCCGCAGCTGCA -3′ and Reverse, 5′-CGGGTTGCCTGCAAAGT -3′; *Clca3* Forward, 5′- AAACGAGAAGGCTTCCATCA-3′ and Reverse, 5′- GGAGATTGCATCGTTGGTTT-3′. Amplification efficiencies were validated and normalized against *ACTB*. Each data point was examined for integrity by analysis of the amplification plot. The mRNA-normalized data were expressed as relative gene mRNA in treated compared to untreated experimental groups or cells.

### Statistical analysis

GraphPad Prism software 6.01 (GraphPad Software) was used for the analysis. Data are expressed as mean ± SD. Horizontal bars indicate the means. Plots of in vivo data are presented as box and whiskers plots; bars represent maximal and minimal values. Statistical significance was calculated by one or two-way ANOVA (Tukey's or Bonferroni's post hoc test) for multiple comparisons and by a two-tailed Student's *t*-test for single comparison. The distribution of levels tested by Kolmogorov-Smirnov normality test turned out to be non-significant. The variance was similar in the groups being compared. We considered all *P* values ≤0.05 significant. The *in vivo* groups consisted of 6 mice/group. The data reported

are either representative of at least three experiments (histology, immunofluorescence, and western blotting) or pooled otherwise.

### Data availability

The data that support the findings of this study are available from the corresponding author upon reasonable request.

## Supplementary Material

Refer to Web version on PubMed Central for supplementary material.

## Acknowledgments

This study was supported by the Specific Targeted Research Project FunMeta (ERC-2011-AdG-293714 to LR). Dr. Marilena Pariano gratefully acknowledges a fellowship from the Italian Cystic Fibrosis Research Foundation. We thank the primary cell culture service offered from the Italian Cystic Fibrosis Research Foundation for kindly providing us with the HBE cells. We thank B. Scholte, Erasmus Medical Center Rotterdam, The Netherlands, who provided *Cftr*$^{tm1EUR}$ (F508del mice, European Economic Community European Coordination Action for Research in Cystic Fibrosis program EU FP6 SHMCT-2005-018932).

## References

1. Rowe SM, Miller S, Sorscher EJ. Cystic fibrosis. N Engl J Med. 2005; 352:1992–2001. [PubMed: 15888700]
2. Lukacs GL, Verkman AS. CFTR: folding, misfolding and correcting the DeltaF508 conformational defect. Trends Mol Med. 2012; 18:81–91. [PubMed: 22138491]
3. Okiyoneda T, et al. Peripheral protein quality control removes unfolded CFTR from the plasma membrane. Science. 2010; 329:805–810. [PubMed: 20595578]
4. Pedemonte N, et al. Small-molecule correctors of defective DeltaF508-CFTR cellular processing identified by high-throughput screening. J Clin Invest. 2005; 115:2564–2571. [PubMed: 16127463]
5. Galietta LJ. Managing the underlying cause of cystic fibrosis: a future role for potentiators and correctors. Paediatr Drugs. 2013; 15:393–402. [PubMed: 23757197]
6. Wainwright CE, Elborn JS, Ramsey BW. Lumacaftor-Ivacaftor in Patients with Cystic Fibrosis Homozygous for Phe508del CFTR. N Engl J Med. 2015; 373:1783–1784.
7. Quon BS, Rowe SM. New and emerging targeted therapies for cystic fibrosis. Bmj. 2016; 352:i859. [PubMed: 27030675]
8. Hegde RN, et al. Unravelling druggable signalling networks that control F508del-CFTR proteostasis. eLife. 2015; 4
9. Tosco A, et al. A novel treatment of cystic fibrosis acting on-target: cysteamine plus epigallocatechin gallate for the autophagy-dependent rescue of class II-mutated CFTR. Cell Death differ. 2016; 23:1380–1393. [PubMed: 27035618]
10. Villella VR, et al. Disease-relevant proteostasis regulation of cystic fibrosis transmembrane conductance regulator. Cell Death differ. 2013; 20:1101–1115. [PubMed: 23686137]
11. Cantin AM, Hartl D, Konstan MW, Chmiel JF. Inflammation in cystic fibrosis lung disease: Pathogenesis and therapy. J Cyst Fibros. 2015; 14:419–430. [PubMed: 25814049]
12. Rubin BK. Cystic fibrosis: myths. mistakes, and dogma. Paediatr Respir Rev. 2014; 15:113–116. [PubMed: 24331762]
13. Cohen TS, Prince A. Cystic fibrosis: a mucosal immunodeficiency syndrome. Nat Med. 2012; 18:509–519. [PubMed: 22481418]
14. Hoffman LR, Ramsey BW. Cystic fibrosis therapeutics: the road ahead. Chest. 2013; 143:207–213. [PubMed: 23276843]

15. de Benedictis FM, Bush A. Corticosteroids in respiratory diseases in children. Am J Respir Crit Care Med. 2012; 185:12–23. [PubMed: 21920920]
16. Devor DC, Schultz BD. Ibuprofen inhibits cystic fibrosis transmembrane conductance regulator-mediated Cl- secretion. J Clin Invest. 1998; 102:679–687. [PubMed: 9710435]
17. Goldstein AL, Goldstein AL. From lab to bedside: emerging clinical applications of thymosin alpha 1. Expert Opin Biol Ther. 2009; 9:593–608. [PubMed: 19392576]
18. Romani L, et al. Thymosin alpha1 activates dendritic cell tryptophan catabolism and establishes a regulatory environment for balance of inflammation and tolerance. Blood. 2006; 108:2265–2274. [PubMed: 16741252]
19. Mandaliti W, et al. New studies about the insertion mechanism of Thymosin alpha1 in negative regions of model membranes as starting point of the bioactivity. Amino Acids. 2016
20. Tuthill CV, King RS. Thymosin Apha 1?A Peptide Immune Modulator with a Broad Range of Clinical Applications. Clin Exp Pharmacol. 2013; 3:1000133.
21. Puccetti P, Grohmann U. IDO and regulatory T cells: a role for reverse signalling and non-canonical NF-kappaB activation. Nat Rev Immunol. 2007; 7:817–823. [PubMed: 17767193]
22. Iannitti RG, et al. Th17/Treg imbalance in murine cystic fibrosis is linked to indoleamine 2,3-dioxygenase deficiency but corrected by kynurenines. Am J Respir Crit Care Med. 2013; 187:609–620. [PubMed: 23306541]
23. Latz E, et al. TLR9 signals after translocating from the ER to CpG DNA in the lysosome. Nat Immunol. 2004; 5:190–198. [PubMed: 14716310]
24. Bruscia E, et al. Isolation of CF cell lines corrected at DeltaF508-CFTR locus by SFHR-mediated targeting. Gene Ther. 2002; 9:683–685. [PubMed: 12032687]
25. King J, Brunel SF, Warris A. *Aspergillus* infections in cystic fibrosis. J Infect. 2016; 72(Suppl):S50–55. [PubMed: 27177733]
26. King RS, Tuthill C. Evaluation of thymosin alpha 1 in nonclinical models of the immune-suppressing indications melanoma and sepsis. Expert Opin Biol Ther. 2015; 15(Suppl 1):S41–49. [PubMed: 25643200]
27. Ancell CD, Phipps J, Young L. Thymosin alpha-1. Am J Health Syst Pharm. 2001; 58:879–885. quiz 886–878. [PubMed: 11381492]
28. Iannitti RG, et al. IL-1 receptor antagonist ameliorates inflammasome-dependent inflammation in murine and human cystic fibrosis. Nat Comm. 2016; 7:10791.
29. Snouwaert JN, et al. An animal model for cystic fibrosis made by gene targeting. Science. 1992; 257:1083–1088. [PubMed: 1380723]
30. Stoltz DA, Meyerholz DK, Welsh MJ. Origins of cystic fibrosis lung disease. N Engl J Med. 2015; 372:351–362. [PubMed: 25607428]
31. McGaha TL. IDO-GCN2 and autophagy in inflammation. Oncotarget. 2015; 6:21771–21772. [PubMed: 26317232]
32. Luciani A, et al. Defective CFTR induces aggresome formation and lung inflammation in cystic fibrosis through ROS-mediated autophagy inhibition. Nat Cell Biol. 2010; 12:863–875. [PubMed: 20711182]
33. Pica F, et al. Serum thymosin alpha 1 levels in patients with chronic inflammatory autoimmune diseases. Clin Exp Immunol. 2016; 186:39–45. [PubMed: 27350088]
34. Denning GM, et al. Processing of mutant cystic fibrosis transmembrane conductance regulator is temperature-sensitive. Nature. 1992; 358:761–764. [PubMed: 1380673]
35. Bomberger JM, Barnaby RL, Stanton BA. The deubiquitinating enzyme USP10 regulates the post-endocytic sorting of cystic fibrosis transmembrane conductance regulator in airway epithelial cells. J Biol Chem. 2009; 284:18778–18789. [PubMed: 19398555]
36. Gentzsch M, et al. Endocytic trafficking routes of wild type and DeltaF508 cystic fibrosis transmembrane conductance regulator. Mol Biol Cell. 2004; 15:2684–2696. [PubMed: 15075371]
37. Sarandeses CS, Covelo G, Diaz-Jullien C, Freire M. Prothymosin alpha is processed to thymosin alpha 1 and thymosin alpha 11 by a lysosomal asparaginyl endopeptidase. J Biol Chem. 2003; 278:13286–13293. [PubMed: 12554742]

38. Heard A, Thompson J, Carver J, Bakey M, Wang XR. Targeting Molecular Chaperones for the Treatment of Cystic Fibrosis: Is It a Viable Approach? Curr Drug Targets. 2015; 16:958–964. [PubMed: 25981601]
39. Millard SM, Wood SA. Riding the DUBway: regulation of protein trafficking by deubiquitylating enzymes. J Cell Biol. 2006; 173:463–468. [PubMed: 16702236]
40. Taillebourg E, et al. The deubiquitinating enzyme USP36 controls selective autophagy activation by ubiquitinated proteins. Autophagy. 2012; 8:767–779. [PubMed: 22622177]
41. Hassink GC, et al. The ER-resident ubiquitin-specific protease 19 participates in the UPR and rescues ERAD substrates. EMBO Rep. 2009; 10:755–761. [PubMed: 19465887]
42. Kucera A, et al. Spatio-temporal resolution of Rab9 and CI-MPR dynamics in the endocytic pathway. Traffic. 2015
43. Lamark T, Johansen T. Autophagy: links with the proteasome. Curr Opin Cell Biol. 2010; 22:192–198. [PubMed: 19962293]
44. Zhang L, et al. CFTR delivery to 25% of surface epithelial cells restores normal rates of mucus transport to human cystic fibrosis airway epithelium. PLoS Biol. 2009; 7:e1000155. [PubMed: 19621064]
45. Van Goor F, et al. Correction of the F508del-CFTR protein processing defect in vitro by the investigational drug VX-809. Proc Natl Acad Sci USA. 2011; 108:18843–18848. [PubMed: 21976485]
46. Yu H, et al. Ivacaftor potentiation of multiple CFTR channels with gating mutations. J Cyst Fibros. 2012; 11:237–245. [PubMed: 22293084]
47. Van Goor F, Yu H, Burton B, Hoffman BJ. Effect of ivacaftor on CFTR forms with missense mutations associated with defects in protein processing or function. J Cyst Fibros. 2014; 13:29–36. [PubMed: 23891399]
48. Caputo A, et al. TMEM16A, a membrane protein associated with calcium-dependent chloride channel activity. Science. 2008; 322:590–594. [PubMed: 18772398]
49. Sala-Rabanal M, Yurtsever Z, Nichols CG, Brett TJ. Secreted CLCA1 modulates TMEM16A to activate Ca(2+)-dependent chloride currents in human cells. eLife. 2015; 4
50. Dalakas MC, Engel WK, McClure JE, Goldstein AL, Askanas V. Immunocytochemical localization of thymosin-alpha 1 in thymic epithelial cells of normal and myasthenia gravis patients and in thymic cultures. J Neurol Sci. 1981; 50:239–247. [PubMed: 7014787]
51. Collawn JF, Matalon S. CFTR and lung homeostasis. Am J Physiol Lung Cell Mol Physiol. 2014; 307:L917–923. [PubMed: 25381027]
52. Yuk JM, Jo EK. Crosstalk between autophagy and inflammasomes. Mol Cells. 2013; 36:393–399. [PubMed: 24213677]
53. Soares MP, Gozzelino R, Weis S. Tissue damage control in disease tolerance. Trends Immunol. 2014; 35:483–494. [PubMed: 25182198]
54. Darrah RJ, et al. Early pulmonary disease manifestations in cystic fibrosis mice. J Cyst Fibros. 2016; 15:736–744. [PubMed: 27231029]
55. van der Doef HP, et al. Association of the CLCA1 p.S357N variant with meconium ileus in European patients with cystic fibrosis. J Pediatr Gastroenterol Nutr. 2010; 50:347–349. [PubMed: 20179644]
56. Young FD, et al. Amelioration of cystic fibrosis intestinal mucous disease in mice by restoration of mCLCA3. Gastroenterology. 2007; 133:1928–1937. [PubMed: 18054564]
57. Clarke LL, et al. Relationship of a non-cystic fibrosis transmembrane conductance regulator-mediated chloride conductance to organ-level disease in *Cftr*($^{-/-}$) mice. Proc Natl Acad Sci USA. 1994; 91:479–483. [PubMed: 7507247]
58. Boyle MP, et al. A CFTR corrector (lumacaftor) and a CFTR potentiator (ivacaftor) for treatment of patients with cystic fibrosis who have a phe508del CFTR mutation: a phase 2 randomised controlled trial. Lancet Respir Med. 2014; 2:527–538. [PubMed: 24973281]
59. Fajac I, De Boeck K. New horizons for cystic fibrosis treatment. Pharmacol Ther. 2016; 170:205–211. [PubMed: 27916649]

60. Pilewski JM, Donaldson SH, Cooke J, Lekstrom-Himes J. Phase 2 studies reveal additive effects of VX-661, an investigational CFTR corrector, and ivacaftor, a CFTR potentiator, in patients who carry the F508del-CFTR mutation. Ped Pulmonol. 2014; 49:157.
61. van Doorninck JH, et al. A mouse model for the cystic fibrosis delta F508 mutation. EMBO J. 1995; 14:4403–4411. [PubMed: 7556083]
62. Tosco A, et al. A novel treatment of cystic fibrosis acting on-target: cysteamine plus epigallocatechin gallate for the autophagy-dependent rescue of class II-mutated CFTR. Cell Death Differ. 2016; 23:1380–1393. [PubMed: 27035618]
63. Iannitti RG, et al. Th17/Treg imbalance in murine cystic fibrosis is linked to indoleamine 2,3-dioxygenase deficiency but corrected by kynurenines. Am J Resp Crit Care Med. 2013; 187:609–620. [PubMed: 23306541]
64. De Stefano D, et al. Restoration of CFTR function in patients with cystic fibrosis carrying the F508del-CFTR mutation. Autophagy. 2014; 10:2053–2074. [PubMed: 25350163]
65. de Luca A, et al. Non-hematopoietic cells contribute to protective tolerance to *Aspergillus fumigatus* via a TRIF pathway converging on IDO. Cell Mol Immunol. 2010; 7:459–470. [PubMed: 20835271]
66. Loffing J, Moyer BD, McCoy D, Stanton BA. Exocytosis is not involved in activation of Cl-secretion via CFTR in Calu-3 airway epithelial cells. Am J Physiol. 1998; 275:C913–920. [PubMed: 9755044]
67. Bruscia E, et al. Isolation of CF cell lines corrected at DeltaF508-CFTR locus by SFHR-mediated targeting. Gene Ther. 2002; 9:683–685. [PubMed: 12032687]
68. Pallotta MT, et al. Indoleamine 2,3-dioxygenase is a signaling protein in long-term tolerance by dendritic cells. Nat Immunol. 2011; 12:870–878. [PubMed: 21804557]
69. Schagger H. Tricine-SDS-PAGE. Nat Protoc. 2006; 1:16–22. [PubMed: 17406207]
70. Sowa ME, Bennett EJ, Gygi SP, Harper JW. Defining the human deubiquitinating enzyme interaction landscape. Cell. 2009; 138:389–403. [PubMed: 19615732]
71. De Luca A, et al. CD4(+) T cell vaccination overcomes defective cross-presentation of fungal antigens in a mouse model of chronic granulomatous disease. J Clin Invest. 2012; 122:1816–1831. [PubMed: 22523066]
72. Munkonge F, et al. Measurement of halide efflux from cultured and primary airway epithelial cells using fluorescence indicators. J Cyst Fibros. 2004; 3(Suppl 2):171–176. [PubMed: 15463953]


Europe PMC Funders Author Manuscripts

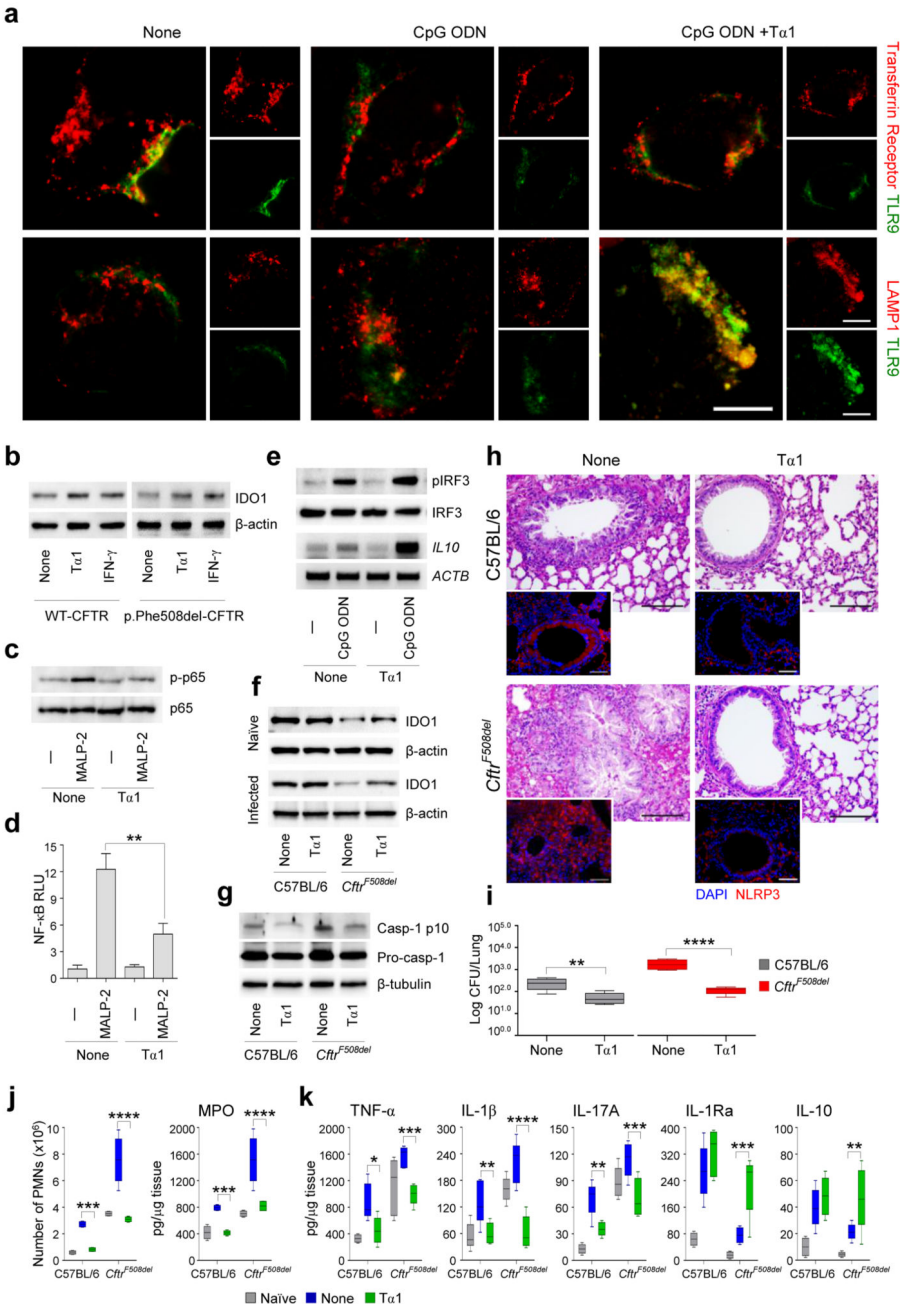


**Figure 1. Tα1 limits the inflammatory response in CF via IDO1.**

(**a**) Representative images ($n$ = 5 images per treatment) of TLR9 co-localization in transferrin receptor$^{+}$ and LAMP-1$^{+}$ positive endosomes in HEK293 cells transfected with human TLR9-GFP stimulated with sub-optimal CpG oligodeoxynucleotides (ODN) with or without 100 ng/ml Tα1. Scale bars, 100 μm. Shown are merged images of cells (single FITC or TRITC images on the right). See Supplementary Fig. 10 for the co-localization coefficients. Representative immunoblot ($n$ = 3) of (**b**) IDO1 protein in WT- or p.Phe508del-CFTR-transfected CFBE41o-cells after treatment with Tα1 or 100 U/ml IFN-γ as a positive




Europe PMC Funders Author Manuscripts

control for 24 h at 37°C; (**c**) NF-KB/p65 (p65), phospho-NF-KB/p65 (p-p65) and (**d**) NF-KB relative luciferase units; (**e**) IRF3 and phospho-IRF3 ($n = 3$) in p.Phe508del-CFTR-transfected CFBE41o-cells cells exposed to MALP-2 or CpG ODN, respectively, in the presence of Tα1 for 2 h. (**e**) *IL10* gene ($n = 3$) expression in cells treated as above. **b**-**g** data are representative of three independent experiments. C57BL/6 or *F508del-Cftr* homozygous ($Cftr^{F508del}$) mice were infected intranasally with live *A. fumigatus* conidia and treated with 200 μg/kg of Tα1 intraperitoneally for 6 days before the lung assessment for: (**f**) IDO1 protein by immunoblotting ($n = 3$); (**g**) caspase-1 cleavage ($n = 3$); (**h**) histology (PAS staining) and immunofluorescence staining with NLRP3 antibody ($n = 5$ images per mouse). Scale bars, 100 μm. (**i**) Fungal growth [$\log_{10}$ colony-forming units (CFU, mean ± SD)]. Immunoblotting and lung sections are representative from three independent experiments with six mice/group. (**j**) Number of PMNs in the BAL and MPO and (**k**) cytokine production in lung homogenates. Assays were done at 7 days post-infection. Data, mean values ± SD, are presented as box-and-whisker plots; bars represent maximal and minimal values. $*P < 0.05$, $**P < 0.01$, $***P < 0.001$, $****P < 0.0001$, Tα1-treated *vs* scrambled peptide-treated (None), –, untreated cells. Two-way ANOVA, Tukey's post test.




Europe PMC Funders Author Manuscripts

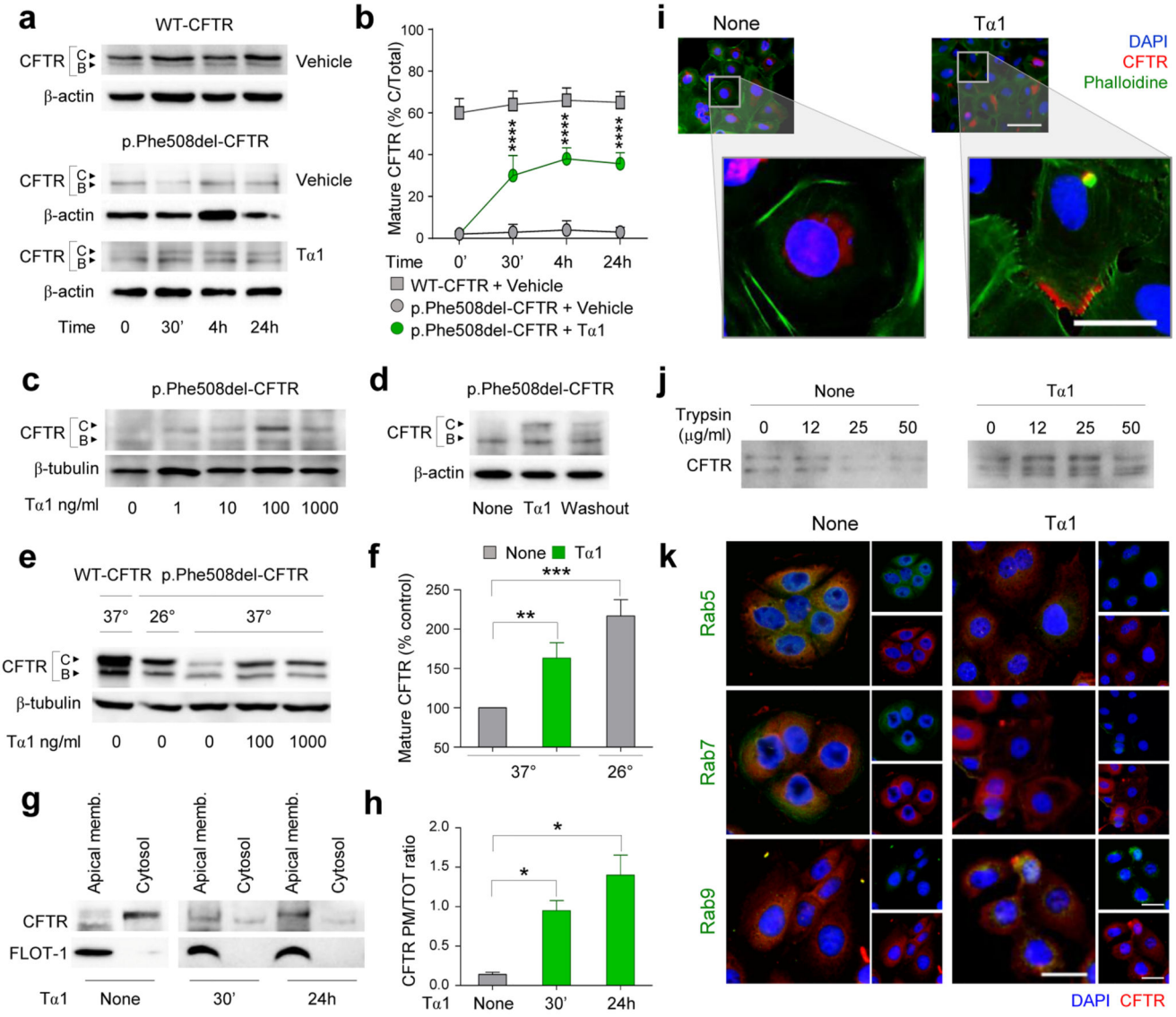


**Figure 2. Tα1 increased cell surface expression and stability of p.Phe508del-CFTR.**

(**a**) CFTR immunoblot ($n = 3$) from WT- or p.Phe508del-CFTR-transfected CFBE41o-cells treated with 100 ng/ml Tα1 or vehicle at various time points. Arrows indicate B and C (mature) forms of CFTR. (**b**) Percentage of band C to total CFTR (B+C) quantified by densitometry. CFTR immunoblot from cells incubated with (**c**) different doses of Tα1 ($n = 3$), (**d**) Tα1 for 24 h ($n = 3$) and after 12 h washout ($n = 3$) and (**e**) Tα1 for 24 h at 26°C or 37°C ($n = 3$) and **(f)** relative percentage of band C to total CFTR (expressed as % of control). (**g**) Immunoblot of purified plasma membranes (PM) with anti-CFTR and FLOT-1 antibodies from cells incubated with Tα1 at 37°C ($n = 3$). (**h**) Fold increase of CFTR at PM on total CFTR. (**i**) Immunofluorescence staining of CFTR ($n = 5$ images per treatment) in cells treated with Tα1 for 24 h. (**j**) Immunoblot of CFTR in cells treated with Tα1 for 24 h 37°C and exposed to trypsin. (**k**) Immunostaining of CFTR with Rab5, Rab7 or Rab9 ($n = 5$ images per treatment) on CFBE41o-cells treated with Tα1 at 37°C for 2 h. Shown are




Europe PMC Funders Author Manuscripts

merged images of cells. See Supplementary Fig. 10 for the co-localization coefficients. (**i** and **k**), scale bars, 100 μm. Immunoblotting and immunofluorescence are representative of three independent experiments. Data are presented as mean ± SD. *$P < 0.05$, **$P < 0.01$, ***$P < 0.001$, ****$P < 0.0001$, Tα1-treated *vs* vehicle (None)-treated cells. Two-way or one-way ANOVA, Tukey's post test.



Europe PMC Funders Author Manuscripts

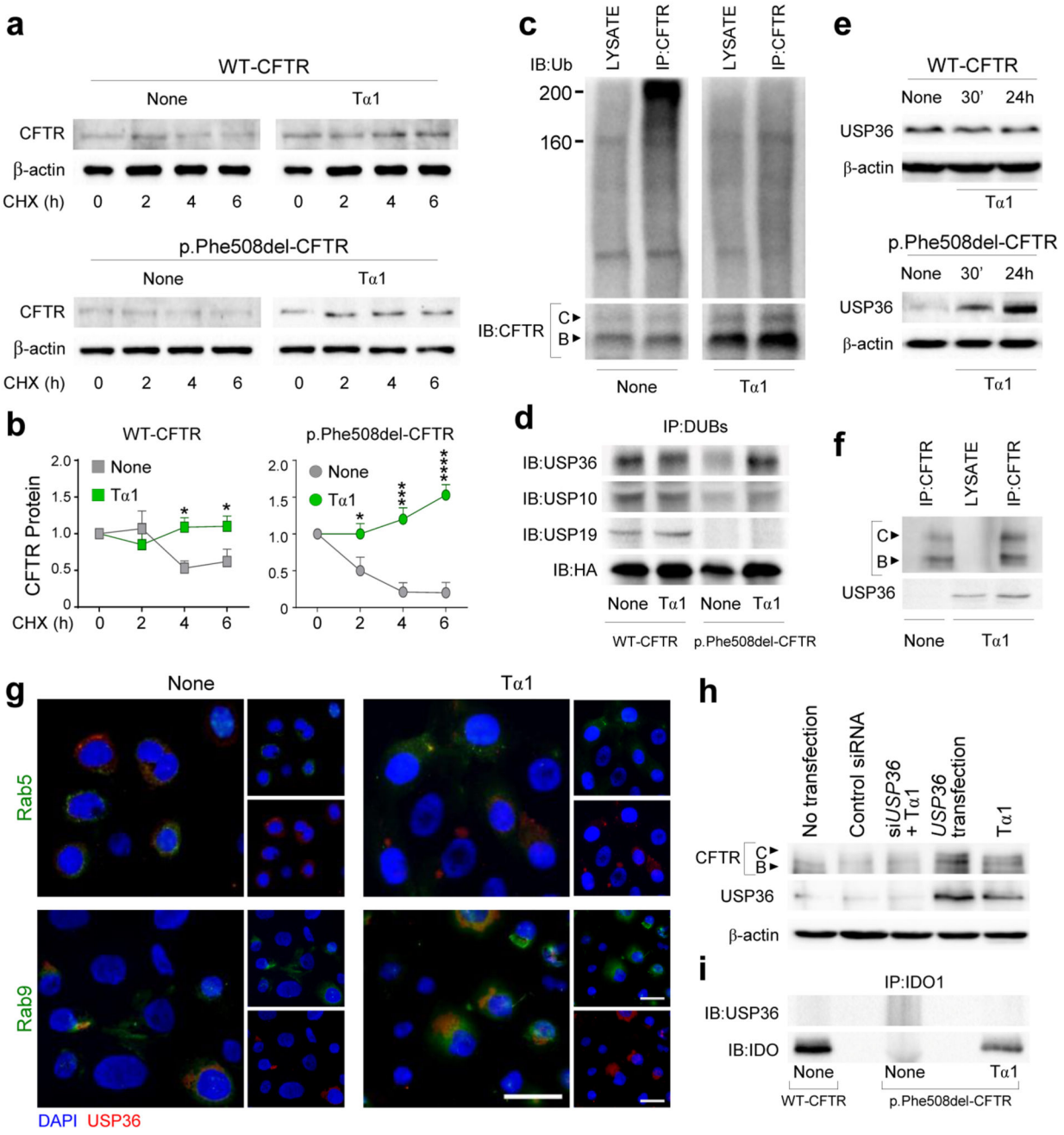


**Figure 3. Tα1 rescues p.Phe508del-CFTR by promoting USP36-deubiquitination.**

(**a**) Immunoblot ($n = 3$) and (**b**) relative densitometric analysis of CFTR in lysates from WT- or p.Phe508del-CFTR-transfected CFBE41o- cells treated with 100 ng/ml Tα1 for 24 h at 37°C and cycloheximide (CHX) for up to 6 h. (**c**) Immunoblot with anti-ubiquitin antibody of total lysates and immunoprecipitated CFTR from cells treated with Tα1 for 2 h ($n = 3$). (**d**) Immunoblotting with anti-HA or anti-USP antibodies ($n = 3$) of lysates from CFBE41o- cells tagged with HA-UbVME. Immunoblot with anti-USP36 of (**e**) total lysates ($n = 3$) or (**f**) immunoprecipitated CFTR ($n = 3$) from cells treated with Tα1 for 30 min or 24 h. (**g**)

Co-localization of USP36 with either Rab5 or Rab9 ($n = 5$ images per treatment) in cell treated with Tα1 for 2 h. Scale bar, 100 μm. See Supplementary Fig. 10 for the co-localization coefficients. (**h**) Immunoblot of CFTR and USP36 ($n = 3$) in cells treated with specific *USP36*, or control, siRNA (scrambled sequence of the siRNA target sequence) or transfected with the plasmid over-expressing *USP36*. (**i**) Immunoblot with anti-USP36 ($n = 3$) on immunoprecipitated IDO1 in cells treated with Tα1 at 37°C for 2 h. Immunoblotting and immunofluorescence are representative of three independent experiments. Data are presented as mean ± SD. $*P < 0.05$, $***P < 0.001$, $****P < 0.0001$, Tα1-treated *vs* vehicle (None)-treated cells. Two-way ANOVA, Bonferroni post test.



Europe PMC Funders Author Manuscripts

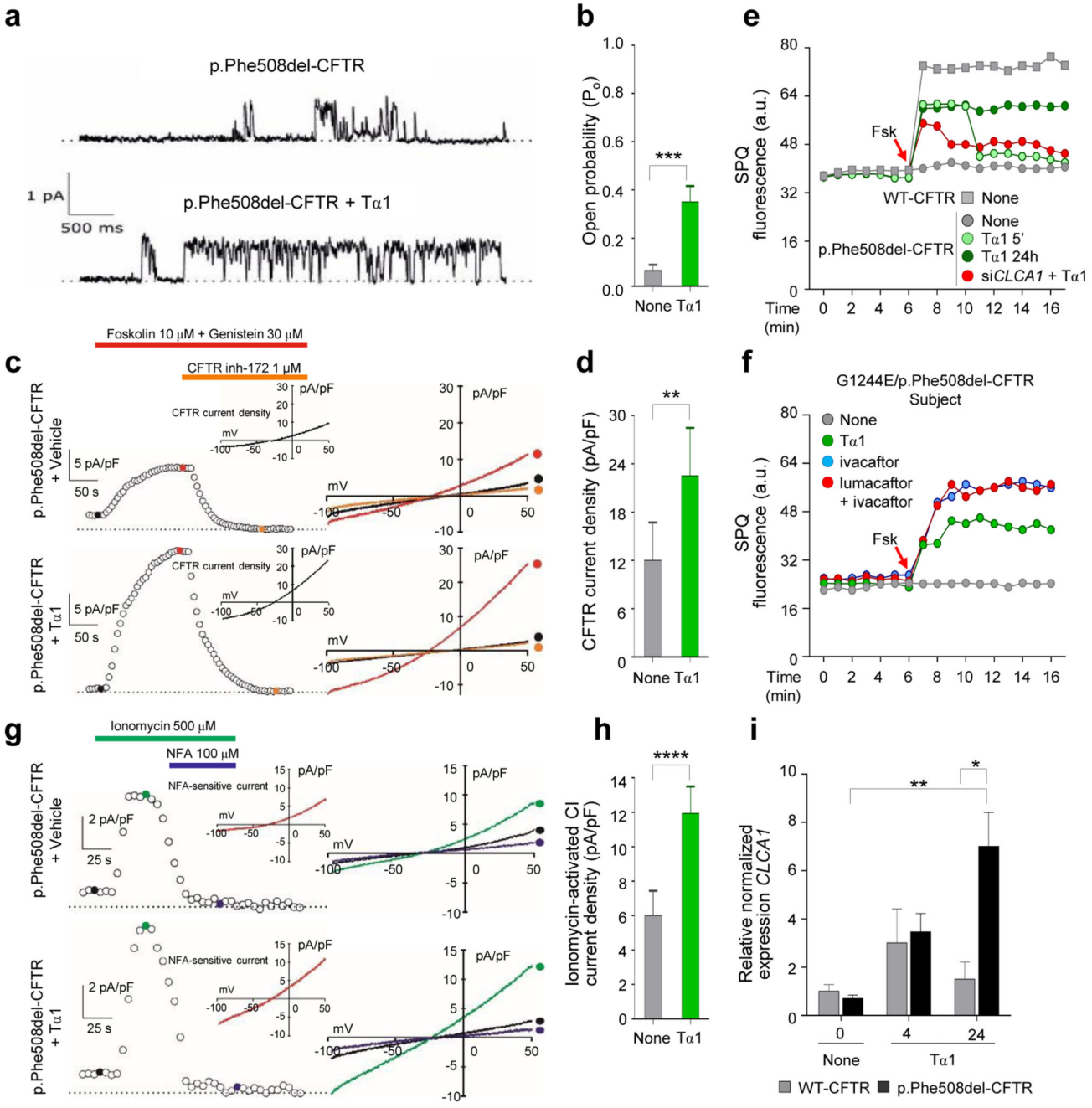


**Figure 4. Tα1 rescues p.Phe508del-CFTR functional activity.**

(**a**) CFTR single-channel currents recorded at +100 mV from p.Phe508del-CFTR-transfected CFBE41o-cells treated with 100 ng/ml Tα1 or vehicle for 2 h (dotted lines indicate the channel's closed state). (**b**) $P_o$ calculated at +100mV ($n = 4$; ***$P < 0.001$; Student's *t*-test). (**c**) Time course of whole-cell CFTR-current densities at +50mV induced by forskolin (Fsk) + Genistein (Gen) in cells treated as above for 24 h (vehicle: top graphs; Tα1: bottom graphs) and followed by blockade with CFTR inh-172. The horizontal bars indicate the time period of drug application (left graphs). I–V relationships elicited by ramps

from -100mV to 50mV (holding potential -40 mV), and constructed at a given time period corresponding to colored dots (right graphs). CFTR inh-172-sensitive chloride current densities were calculated by subtracting from Fsk+Gen-induced current density the residual current density recorded after the application of CFTR inh-172 (insets). (**d**) Average Fsk +Gen-induced CFTR-current density ($n = 8$; $^{**}P < 0.01$; Student's t-test). (**e**) Iodide efflux by a fluorescence assay (SPQ) upon stimulation with Fsk in cells treated with Tα1 at 37°C ($n = 3$). *CLCA1,* or control, siRNA was performed 24 h before Tα1 addition for 5 min only. (**f**) Iodide efflux in cells treated with Tα1 or ivacaftor alone or in combination with lumacaftor for 24 h at 37°C ($n = 3$). (**g**) Time course of ionomycin-induced calcium-activated chloride current densities at +50mV in cells treated and depicted as in **c**, followed by blockade with niflumic acid (NFA) 100 μM (left graphs). I–V relationships elicited and depicted as in **c** (right graphs). NFA-sensitive chloride current densities were calculated by subtracting from ionomycin-induced current density the residual current density recorded after the application of NFA 100 μM (insets). (**h**) Average current density ($n = 8$; $^{****}P < 0.0001$; Student's *t*-test). (**i**) *CLCA1* expression by RT-PCR in cells treated with Tα1 at 37°C ($n = 5$). Data are presented as mean ± SD. $^{*}P < 0.05$, $^{**}P < 0.01$, treated *vs* vehicle alone (None) cells; p.Phe508del-CFTR-transfected *vs* WT-CFTR-transfected cells. Two-way ANOVA, Bonferroni post test. None, vehicle-treated cells. For statistical analysis, see Supplementary Fig. 10.

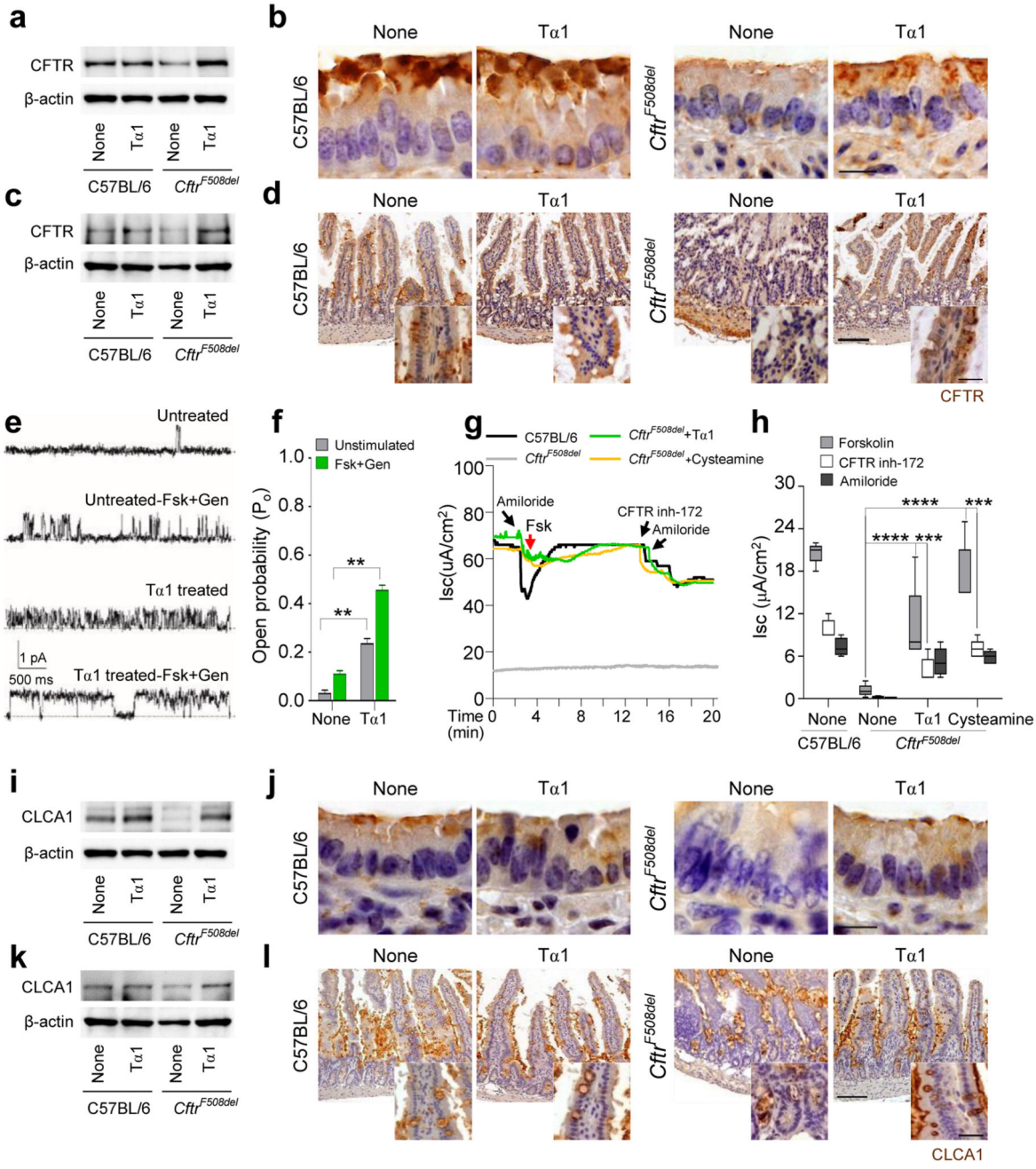


**Figure 5. Tα1 rescues p.Phe508del-CFTR activity in *Cftr*$^{F508del}$ mice.**

C57BL/6 or *F508del-Cftr* homozygous (*Cftr*$^{F508del}$) mice were treated with 200 μg/kg of Tα1 intraperitoneally for 6 days before the assessment of CFTR protein expression in lung (**a**, **b**) and small intestine (**c**, **d**) by immunoblotting of lysates ($n = 3$) (**a, c**) and immunohistochemistry ($n = 5$ images per mice) (**b**, **d**). Scale bars, 25 μm in **b**; 200 μm in **d** and 100 μm in the inset. (**e**) CFTR single-channel currents recorded at + 100 mV from ex-vivo purified epithelial cells in response to forskolin (Fsk) + Genistein (Gen) ($n = 4$) (dotted lines give the zero current baseline when the channel is in its closed state). (**f**) $P_o$ of channels

calculated at +100mV ($n = 4$). (**g**) CFTR-dependent $Cl^-$ secretion ($n = 4$) measured by means of Fsk-induced increase of the chloride current (Isc ($\mu A/cm^2$) (summarized in **h**) in ex-vivo ileum mounted in Ussing chambers in the presence of CFTR inhibition (CFTR inh-172) and amiloride. Cysteamine was used as positive control. CLCA1 protein expression in lung (**i, j**) and small intestine (**k**, **l**) by immunoblotting of lysates ($n = 3$) (**i**, **k**) and immunohistochemistry ($n = 5$ images per mice) (**j**, **l**). Scale bars, 25 μm in **j**; 200 μm in **l**, 100 μm in the inset. Immunoblotting and immunohistochemical sections are representative of three independent experiments with 6 mice/group. Data are presented as mean ± SD. $^{**}P < 0.01$, $^{***}P < 0.001$, $^{****}P < 0.0001$, Tα1- or cysteamine-treated *vs* scrambled peptide-treated (None) mice. Two-way ANOVA, Bonferroni post test.

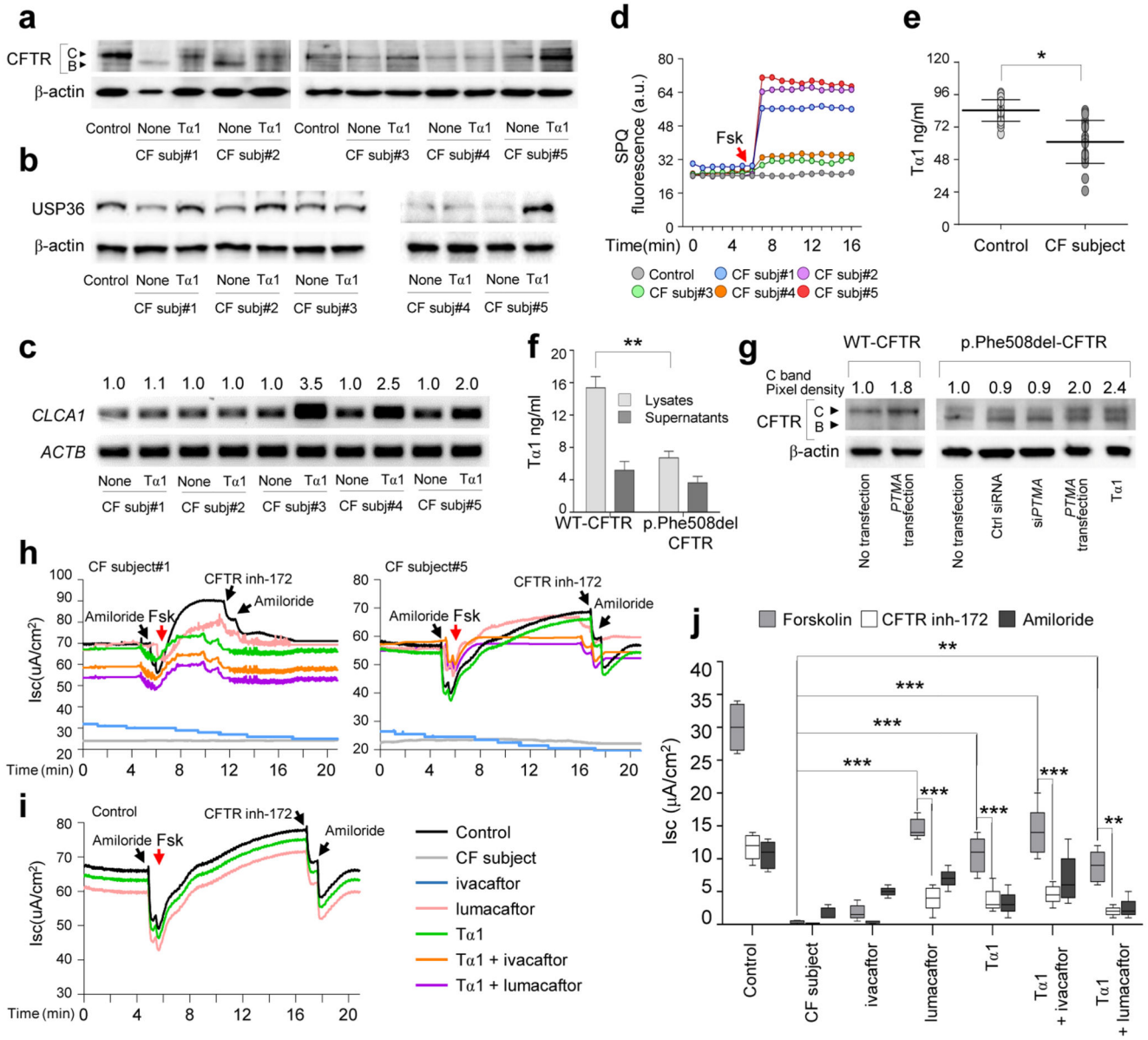


**Figure 6. Tα1 rescues p.Phe508del-CFTR activity in CF cells and HBE cells from subjects with CF.**

CFTR (**a**) and USP36 (**b**) protein expression ($n = 3$); (**c**) *CLCA1* gene expression ($n = 3$) and (**d**) iodide efflux by SPQ upon stimulation with forskolin (Fsk) in HBE cells from 5 subjects (subj) with the p.Phe508del mutation and controls treated with 100 ng/ml Tα1 for 24 h at 37°C. Tα1 production on (**e**) sputa from controls and subjects with CF ($n = 3$; $^*P < 0.05$ subjects with CF *vs* controls, Student's *t*-test) and (**f**) lysates or supernatants from WT- or p.Phe508del-CFTR-transfected CFBE41o-cells ($n = 3$; $^{**}P < 0.01$ p.Phe508del-CFTR- *vs* WT-CFTR-transfected cells, two-way ANOVA, Bonferroni post test). (**g**) Immunoblot of CFTR and C band pixel density ($n = 3$) in cells transfected with prothymosin (*PTMA*) siRNA or the plasmid over expressing *PTMA* and treated with Tα1 at 37°C for 2 h.

Immunoblotting are representative from three independent experiments. CFTR-dependent $Cl^-$ secretion ($n = 4$) measured by means of forskolin-induced increase of the chloride current (Isc ($\mu A/cm^2$) in HBE cells from two (**h**) subjects with CF or (**i**) controls (summarized in **j**) treated with Tα1, ivacaftor or lumacaftor for 24 h at 37°C and mounted in Ussing chambers in the presence of CFTR inhibition (CFTR inh-172) and amiloride. Data are presented as mean ± SD. $^{**}P < 0.01$, $^{***}P < 0.001$, p.Phe508del-CFTR- *vs* WT-CFTR-transfected cells, two-way ANOVA, Bonferroni post test.



Europe PMC Funders Author Manuscripts